Quantum dynamics of a two-level system coupled to a shape-invariant potential

2005 J. Phys. A: Math. Gen. 38 8603

(http://iopscience.iop.org/0305-4470/38/40/009)

INSTITUTE OF PHYSICS PUBLISHING JOURNAL OF PHYSICS A: MATHEMATICAL AND GENERAL

J. Phys. A: Math. Gen. **38** (2005) 8603–8631 doi:10.1088/0305-4470/38/40/009

Quantum dynamics of a two-level system coupled to a shape-invariant potential

A N F Aleixo[1] **and A B Balantekin**[2]

[1] Instituto de Física, Universidade Federal do Rio de Janeiro, RJ, Brazil
[2] Department of Physics, University of Wisconsin, Madison, WI 53706, USA

E-mail: armando@if.ufrj.br and baha@physics.wisc.edu

Received 8 May 2005, in final form 30 August 2005
Published 21 September 2005
Online at stacks.iop.org/JPhysA/38/8603

Abstract

The quantum dynamics of a two-level system coupled to a shape-invariant potential is investigated. Shape-invariant potentials share an integrability condition called shape invariance which identifies an underlying algebraic structure, in general infinite dimensional, that transforms the potential parameters such as strength, range and diffuseness. We determine the time-evolution operator, the density operator of the system, and obtain the temporal behaviour of various dynamical variables by considering either pure or mixed initial states of the system, constructed with the generalized coherent state of the shape-invariant coupling potential. We consider specific examples of shape-invariant coupling potentials (harmonic oscillator, Pöschl–Teller and self-similar potentials). The results obtained for all dynamical variables exhibit rapid oscillations which periodically collapse and regenerate in different ways depending on the coupling potential nature.

PACS numbers: 03.65.−w, 03.65.Ge, 03.65.Fd

1. Introduction

Supersymmetric quantum mechanics [1] is usually studied in the context of one-dimensional systems. The partner Hamiltonians

$$\hat{H}_1 = -\frac{\hbar^2}{2m}\frac{\mathrm{d}^2}{\mathrm{d}x^2} + V_-(x) = \hbar\Omega\,\hat{A}^\dagger\hat{A} \qquad \text{and} \qquad \hat{H}_2 = -\frac{\hbar^2}{2m}\frac{\mathrm{d}^2}{\mathrm{d}x^2} + V_+(x) = \hbar\Omega\,\hat{A}\hat{A}^\dagger \tag{1.1}$$

can be written in terms of one-dimensional operators

$$\hat{A} \equiv \frac{1}{\sqrt{\hbar\Omega}}\left(W(x) + \frac{\mathrm{i}}{\sqrt{2m}}\hat{p}\right) \qquad \text{and} \qquad \hat{A}^\dagger \equiv \frac{1}{\sqrt{\hbar\Omega}}\left(W(x) - \frac{\mathrm{i}}{\sqrt{2m}}\hat{p}\right) \tag{1.2}$$

where $\hbar\Omega$ is a constant energy scale factor, introduced so that the operators $\hat{A}$ and $\hat{A}^\dagger$ are dimensionless, and $W(x)$ is the superpotential which is related to the potentials $V_\pm(x)$ via

$$V_\pm(x) = W^2(x) \pm \frac{\hbar}{\sqrt{2m}} \frac{\mathrm{d}W(x)}{\mathrm{d}x}. \tag{1.3}$$

A number of such pairs of Hamiltonians $\hat{H}_{1,2}$ share an integrability condition called shape invariance [2]. Although not all exactly-solvable problems are shape-invariant [3], shape invariance, especially in its algebraic formulation [4–6], proved to be a powerful technique to investigate exactly-solvable systems. Previous attempts to generalize supersymmetric quantum mechanics and the concept of shape invariance beyond one-dimensional and spherically-symmetric three-dimensional problems include non-central [7], non-local [8] and periodic [9] potentials; a three-body problem in one dimension [10] with a three-body force [11]; N-body problem [12] and coupled-channel problems [13, 14].

In earlier publications [15, 16] we introduced a class of coupled-channel problems which generalize the Jaynes–Cummings Hamiltonian [17], a simple model which is extensively used in quantum optics where the radiation, represented by a harmonic oscillator, is coupled to an atom, represented by a two-level system. A two-level system may approximate a number of interesting physical situations [18]. For such an approach to be operable the system in consideration should have two states whose energies are close together and sufficiently different from all the other energy levels of the system. Under these conditions, if we want to evaluate the effect of a sufficiently weak external perturbation on these two states, to a first approximation, we can ignore all the other energy levels of the system and perform the calculations in a two-dimensional subspace of the energy state space [19]. The field of the quantum optics is the best-known example of the success of this procedure.

In the present paper, we study the quantum dynamics of a class of coupled-channel problems where a two-level system is coupled to a shape-invariant potential. We consider two possible forms of coupling: a constant coupling and an intensity-dependent coupling. Using other shape-invariant potentials besides the harmonic oscillator leads to non-trivial coupled-channel problems which may find applications in molecular, atomic or nuclear physics. Being exactly solvable, our model may help in assessing the validity and accuracy of various approaches to coupled-channel problems. In this context, we obtain the explicit expressions for the time-evolution operator and the density operator.

We use generalized coherent states associated with shape-invariant potentials, obtained in a previous study [20], to construct either a pure or a mixed initial state of the system. We then evaluate the expectation values of various dynamical variables of the system, such as the population inversion factor, the intensity of the shape-invariant coupling (usually called the excitation number) and the Mandel parameter, which represents deviations of the state of the system from the coherent state.

This paper is organized as follows: in section 2 we review the algebraic formulation of the shape invariance; in section 3 we present the Hamiltonian for a two-level system coupled to a general shape-invariant potential and obtain the eigenstates of that system; in section 4 we introduce the density operator formalism for the two-level coupled system and obtain the expression for the density matrix as a function of the time considering pure or mixed initial states; in section 5 we apply the density operator formalism to obtain the expectation values of the dynamical variables cited above and in section 6 we apply our generalized result for three different kinds of coupling potentials (the harmonic oscillator, the Pöschl–Teller and the self-similar potentials) and discuss the behaviour of the dynamical variables for each system. Finally, a conclusion and brief remarks close the paper in section 7.

2. Algebraic formulation and coherent states for shape-invariant systems

The Hamiltonian $\hat{H}_1$ of equation (1.1) is called shape-invariant if the condition,

$$\hat{A}(a_1)\hat{A}^\dagger(a_1) = \hat{A}^\dagger(a_2)\hat{A}(a_2) + R(a_1), \tag{2.1}$$

is satisfied [2]. In this equation a_1 and a_2 represent a set of parameters that specify space-independent properties of the potentials (such as strength, range and diffuseness). The parameter a_2 is a function of a_1 and the remainder $R(a_1)$ is independent of the dynamical variables such as position and momentum. As it is written the condition of equation (2.1) does not require the Hamiltonian to be one-dimensional, and one does not need to choose the ansatz of equation (1.2). In the cases studied so far the parameters a_1 and a_2 are either related by a translation [3, 21] $a_n = a_1 + (n-1)\eta$ or a scaling [6, 20, 22] $a_n = a_1 q^{n-1}$ with $n \in \mathbb{Z}$. Concrete examples for shape-invariant condition of equation (2.1) are presented in the cited references. Introducing the operator $\hat{T} \equiv \hat{T}(a_1)$ and the similarity transformation $\hat{T}\hat{O}(a_1)\hat{T}^\dagger = \hat{O}(a_2)$ that replace a_1 with a_2 in a given operator $\hat{O}(a_1)$ [4, 6] and the operators

$$\hat{B}_+ = \hat{A}^\dagger(a_1)\hat{T} \qquad \text{and} \qquad \hat{B}_- = \hat{B}_+^\dagger = \hat{T}^\dagger\hat{A}(a_1), \tag{2.2}$$

the Hamiltonians of equation (1.1) take the forms $\hat{H}_1 = \hbar\Omega\hat{B}_+\hat{B}_-$ and $\hat{H}_2 = \hbar\Omega\hat{T}\hat{B}_-\hat{B}_+\hat{T}^\dagger$. As is shown in [4], with equation (2.1) one can also easily prove the commutation relation $[\hat{B}_-, \hat{B}_+] = \hat{T}^\dagger R(a_1)\hat{T} \equiv R(a_0)$, where we used the identity $R(a_n) = \hat{T}R(a_{n-1})\hat{T}^\dagger$, valid for any $n \in \mathbb{Z}$. This commutation relation suggests that $\hat{B}_-$ and $\hat{B}_+$ are the appropriate creation and annihilation operators for the spectra of the shape-invariant potentials provided that their non-commutativity with $R(a_1)$ is taken into account. The additional relations

$$R(a_n)\hat{B}_+ = \hat{B}_+R(a_{n-1}) \qquad \text{and} \qquad R(a_n)\hat{B}_- = \hat{B}_-R(a_{n+1}), \tag{2.3}$$

readily follow from these results. Considering that the ground state of the Hamiltonian $\hat{H}_1$ satisfies the condition $\hat{A}|0\rangle = 0 = \hat{B}_-|0\rangle$, then, using the above relations it is possible to find the nth excited state of $\hat{H}_1$

$$\hat{H}_1|n\rangle \equiv \hbar\Omega(\hat{B}_+\hat{B}_-)|n\rangle = \hbar\Omega\, e_n|n\rangle \qquad \text{and} \qquad \hat{B}_-\hat{B}_+|n\rangle = \{e_n + R(a_0)\}|n\rangle \tag{2.4}$$

where these eigenstates can be written in a normalized form as

$$|n\rangle = \frac{1}{\sqrt{R(a_1)+R(a_2)+\cdots+R(a_n)}}\hat{B}_+\cdots\frac{1}{\sqrt{R(a_1)+R(a_2)}}\hat{B}_+\frac{1}{\sqrt{R(a_1)}}\hat{B}_+|0\rangle \tag{2.5}$$

with the eigenvalues $\mathcal{E}_n = \hbar\Omega\, e_n$, with $e_0 = 0$ and

$$e_n = \sum_{k=1}^{n} R(a_k), \qquad \text{for} \quad n \geqslant 1. \tag{2.6}$$

Coherent states [23] are quantum-mechanical states which provide a close connection between quantum and classical formulations of a given physical system. Based on the Heisenberg–Weyl group and applied specifically to harmonic oscillator system, the original coherent state introduced by Schrödinger has been extended to a large number of Lie groups with square integrable representations [23]. Today these extensions are used in many applications in a number of contexts, especially in quantum optics and radiophysics. In a previous work [24], we showed that the coherent states for shape-invariant systems with an infinite number of energy levels can be obtained in a generalized way:

$$|z; a_j\rangle = \sum_{n=0}^{\infty}\{z\mathcal{Z}_j\hat{B}_-^{-1}\}^n|0\rangle, \qquad z, \mathcal{Z}_j \in \mathbb{C}, \tag{2.7}$$

where the right inverse operator for $\hat{B}_-$ is defined by the relation $\hat{B}_-^{-1} = \hat{\mathcal{H}}^{-1}\hat{B}_+$ with $\hat{\mathcal{H}} \equiv \hat{B}_+\hat{B}_-$, and we used the shorthand notation $\mathcal{Z}_j \equiv \mathcal{Z}(a_1, a_2, a_3, \ldots)$ for an arbitrary functional of the potential parameters, introduced to establish a more general approach. With the relation (2.3) we can prove that this coherent state is the eigenstate of the operator $\hat{B}_-$ since

$$\hat{B}_-|z; a_j\rangle = z\mathcal{Z}_{j-1}|z; a_j\rangle, \tag{2.8}$$

where $\mathcal{Z}_{j-1} = \hat{T}^\dagger\mathcal{Z}_j\hat{T} = \mathcal{Z}(a_0, a_1, a_2, \ldots)$. In a non-normalized Glauber's form [25], this coherent state can be written in terms of the eigenstates of the Hamiltonian $\hat{H}_1$ as [24]

$$|z; a_r\rangle = \sum_{n=0}^{\infty} \frac{z^n}{h_n(a_r)}|n\rangle, \tag{2.9}$$

where we used the shorthand notation $h_n(a_r) \equiv h_n[a_1, a_2, \ldots, a_n]$ for the expansion coefficients, which are given by $h_0(a_r) = 1$ and

$$h_n(a_r) = \prod_{s=0}^{n-1}\left[\frac{\sqrt{e_n - e_s}}{\mathcal{Z}_{j+s}}\right], \qquad \text{for} \quad n \geqslant 1, \tag{2.10}$$

with e_n given by equation (2.6) and $\mathcal{Z}_{j+s} = \hat{T}^s\mathcal{Z}_j\hat{T}^{\dagger s} = \mathcal{Z}(a_{1+s}, a_{2+s}, a_{3+s}, \ldots)$. The generalized coherent state in (2.9) possesses the basic requirements necessary for a close connection between classical and quantum formulations of a given system [24], such as label continuity, the resolution of unity, temporal stability and the action identity.

3. A two-level system coupled to a shape-invariant potential

3.1. Hamiltonian

In treating two-level systems it is often handy to use a 2×2 matrix notation. The Hamiltonian that describes the coupling of a two-level system with a shape-invariant potential can be decomposed in the following form,

$$\hat{\mathbf{H}} = \hat{\mathbf{H}}_0 + \hat{\mathbf{H}}_{\text{int}}^{(\text{x})}, \tag{3.1}$$

where

$$\hat{\mathbf{H}}_0 = \hbar\Omega\,\hat{\mathbf{S}}^2, \qquad \text{with} \quad \hat{\mathbf{S}} = \hat{\sigma}_+\hat{A} + \hat{\sigma}_-\hat{A}^\dagger, \tag{3.2}$$

and the operators $\hat{A}$ and $\hat{A}^\dagger$ satisfy the shape invariance condition of equation (2.1). In this study, we consider two possible forms for the interaction Hamiltonian,

$$\hat{\mathbf{H}}_{\text{int}}^{(\text{u})} = \hbar\lambda(\hat{\mathbf{S}} + \Delta\hat{\sigma}_3) \qquad \text{and} \qquad \hat{\mathbf{H}}_{\text{int}}^{(\text{i})} = \hbar\lambda(\hat{\mathbf{K}}^\dagger\,\hat{\mathbf{S}}\,\hat{\mathbf{K}} + \Delta\hat{\sigma}_3), \tag{3.3}$$

where $\hat{\mathbf{K}} = \hat{\mathbf{K}}^\dagger = \frac{1}{2}[(\hat{\mathbf{1}} + \hat{\sigma}_3) + (\hat{\mathbf{1}} - \hat{\sigma}_3)\sqrt{\hat{A}^\dagger\hat{A}}]$. The expressions for $\hat{\mathbf{H}}_{\text{int}}^{(\text{u})}$ and $\hat{\mathbf{H}}_{\text{int}}^{(\text{i})}$ represent the constant (x = u) [17] and intensity-dependent (x = i) [26] couplings, respectively. In these equations λ is a constant related to the coupling strength, Δ is a constant related to the detuning of the system and the two-level flip operators are defined by $\hat{\sigma}_\pm = \frac{1}{2}(\hat{\sigma}_1 \pm \mathrm{i}\hat{\sigma}_2)$, where $\hat{\sigma}_i$, for $i = 1, 2$ and 3, are the Pauli matrices. Note that for the harmonic oscillator potential, the simplest shape-invariant potential, we have the standard and intensity-dependent versions of the Jaynes–Cummings model, which is of fundamental importance for the field of the quantum optics.

The algebraic formulation presented in section 2 can be applied in the Hamiltonian (3.1) by using the $\hat{B}_\pm$ operators introduced by equation (2.2). If we define the matrix

$$\hat{\mathbf{T}} = \tfrac{1}{2}[(\hat{\mathbf{1}} + \hat{\sigma}_3)\hat{T} + (\hat{\mathbf{1}} - \hat{\sigma}_3)] \tag{3.4}$$

and decompose the Hamiltonian $\hat{\mathbf{h}}$ in

$$\hat{\mathbf{h}} = \hat{\mathbf{h}}_0 + \hat{\mathbf{h}}_{\rm int}^{(\rm x)}, \tag{3.5}$$

with

$$\hat{\mathbf{h}}_0 = \hbar\Omega\,\hat{\mathbf{s}}^2, \qquad \text{and} \qquad \hat{\mathbf{s}} = \hat{\sigma}_+\hat{B}_- + \hat{\sigma}_-\hat{B}_+, \tag{3.6}$$

the final result can be written as

$$\hat{\mathbf{H}} = \hat{\mathbf{T}}\hat{\mathbf{h}}\hat{\mathbf{T}}^\dagger. \tag{3.7}$$

The interaction Hamiltonian $\hat{\mathbf{h}}_{\rm int}^{(\rm x)}$ can be written as

$$\hat{\mathbf{h}}_{\rm int}^{(\rm u)} = \hbar\lambda(\hat{\mathbf{s}} + \Delta\hat{\sigma}_3) \qquad \text{and} \qquad \hat{\mathbf{h}}_{\rm int}^{(\rm i)} = \hbar\lambda(\hat{\mathbf{k}}^\dagger\hat{\mathbf{s}}\,\hat{\mathbf{k}} + \Delta\hat{\sigma}_3), \tag{3.8}$$

with the $\hat{\mathbf{k}}$ matrix given by $\hat{\mathbf{k}} = \hat{\mathbf{k}}^\dagger = \frac{1}{2}[(\hat{\mathbf{1}} + \hat{\sigma}_3) + (\hat{\mathbf{1}} - \hat{\sigma}_3)\sqrt{\hat{B}_+\hat{B}_-}]$. In writing these expressions we used definition (3.3) and the unitary property $\hat{T}^\dagger\hat{T} = \hat{T}\hat{T}^\dagger = \hat{1}$.

3.2. Eigenstates and eigenvalues

As shown in [15, 16], the eigenstates of $\hat{\mathbf{H}}$, obtained from the solution of the eigenvalue equation

$$\hat{\mathbf{H}}|\Psi_n\rangle = E_n|\Psi_n\rangle, \tag{3.9}$$

are given by

$$\left|\Psi_0^{(\pm)}\right\rangle = \begin{bmatrix} 0 \\ |0\rangle \end{bmatrix}, \qquad \left|\Psi_n^{(\pm)}\right\rangle = \begin{bmatrix} \hat{T}(a_1)N_n^{(\pm)}|n\rangle \\ \pm N_{n+1}^{(\pm)}|n+1\rangle \end{bmatrix}, \qquad n = 1, 2, 3, \ldots, \tag{3.10}$$

where $N_{n,n+1}^{(\pm)} \equiv N_{n,n+1}^{(\pm)}[R(a_1), R(a_2), R(a_3), \ldots]$ are auxiliary normalization coefficients which are related by the constraint $N_{n+1}^{(\pm)} = N_n^{(\mp)}$. In the resonant limit ($\Delta = 0$) it is possible to show that $N_n^{(\pm)} = N_{n+1}^{(\pm)} = 1/\sqrt{2}$. Depending on the coupling interaction form, the corresponding eigenvalues are given by

$$E_n^{(\pm)} = \hbar\Omega e_{n+1} \pm \hbar\lambda \begin{cases} \sqrt{e_{n+1} + \Delta^2} & \text{for} \quad \text{x} = \text{u}; \\ \sqrt{e_{n+1}^2 + \Delta^2} & \text{for} \quad \text{x} = \text{i}. \end{cases} \tag{3.11}$$

3.3. Time evolution operator

By using the Hamiltonian (3.1) presented above we can write the Schrödinger equation for a two-level system coupled with a shape-invariant potential as

$$\hat{\mathbf{H}}|\Psi(t)\rangle = \mathrm{i}\hbar\frac{\partial}{\partial t}|\Psi(t)\rangle, \qquad \text{where} \quad |\Psi(t)\rangle = \begin{bmatrix} |\Psi_\alpha(t)\rangle \\ |\Psi_\beta(t)\rangle \end{bmatrix}. \tag{3.12}$$

Introducing the wavefunction $|\psi(t)\rangle$ by $|\Psi(t)\rangle = \hat{\mathbf{T}}|\psi(t)\rangle$ and using it in equations (3.12) we find

$$\hat{\mathbf{h}}|\psi(t)\rangle = \mathrm{i}\hbar\frac{\partial}{\partial t}|\psi(t)\rangle, \tag{3.13}$$

where we used the unitary matrix property $\hat{\mathbf{T}}\hat{\mathbf{T}}^\dagger = \hat{\mathbf{T}}^\dagger\hat{\mathbf{T}} = \hat{\mathbf{1}}$. If we write the wavefunction $|\psi(t)\rangle$ as

$$|\psi(t)\rangle = \exp(-\mathrm{i}\hat{\mathbf{h}}_0 t/\hbar)|\psi_i(t)\rangle, \tag{3.14}$$

and use it in (3.13) with the commutation property between $\hat{\mathbf{h}}_0$ and $\hat{\mathbf{h}}_{\rm int}^{(\rm x)}$, we obtain

$$\hat{\mathbf{h}}_{\rm int}^{(\rm x)}|\psi_i(t)\rangle = \mathrm{i}\hbar\frac{\partial}{\partial t}|\psi_i(t)\rangle. \tag{3.15}$$

Defining the time-evolution operator $\hat{\mathbf{u}}_i(t,0)$ for the interaction Hamiltonian $\hat{\mathbf{h}}_{\rm int}^{(\rm x)}$ by $|\psi_i(t)\rangle = \hat{\mathbf{u}}_i(t,0)|\psi_i(0)\rangle$, and using it in equation (3.15) it is possible to find

$$\hat{\mathbf{h}}_{\rm int}^{(\rm x)}\hat{\mathbf{u}}_i(t,0) = \mathrm{i}\hbar\frac{\partial}{\partial t}\hat{\mathbf{u}}_i(t,0). \tag{3.16}$$

To diagonalize this time-evolution matrix differential equation one can differentiate equation (3.16) with respect to time once more. We find

$$\frac{\partial^2}{\partial t^2}\hat{\mathbf{u}}_i(t,0) + \frac{1}{\hbar^2}\big[\hat{\mathbf{h}}_{\rm int}^{(\rm x)}\big]^2\hat{\mathbf{u}}_i(t,0) = \mathbf{0}, \tag{3.17}$$

which, in a matrix form, can be written as

$$\begin{bmatrix}\hat{u}''_{11} & \hat{u}''_{12}\\ \hat{u}''_{21} & \hat{u}''_{22}\end{bmatrix} + \begin{bmatrix}\hat{\omega}^2_{\rm x1} & 0\\ 0 & \hat{\omega}^2_{\rm x2}\end{bmatrix}\begin{bmatrix}\hat{u}_{11} & \hat{u}_{12}\\ \hat{u}_{21} & \hat{u}_{22}\end{bmatrix} = \mathbf{0}, \tag{3.18}$$

where the primes denote the time derivative and

$$\begin{cases}\hat{\omega}_{\rm u1} = \lambda\sqrt{\hat{B}_-\hat{B}_+ + \Delta^2}, & \hat{\omega}_{\rm u2} = \lambda\sqrt{\hat{B}_+\hat{B}_- + \Delta^2}, \qquad \text{for} \quad \mathrm{x} = \mathrm{u};\\ \hat{\omega}_{\rm i1} = \lambda\sqrt{(\hat{B}_-\hat{B}_+)^2 + \Delta^2}, & \hat{\omega}_{\rm i2} = \lambda\sqrt{(\hat{B}_+\hat{B}_-)^2 + \Delta^2}, \qquad \text{for} \quad \mathrm{x} = \mathrm{i}.\end{cases} \tag{3.19}$$

Since by initial conditions $\hat{\mathbf{u}}_i(0,0) = \hat{\mathbf{1}}$, and, also by the unitarity conditions we must have $\hat{\mathbf{u}}_i^\dagger(t,0)\hat{\mathbf{u}}_i(t,0) = \hat{\mathbf{u}}_i(t,0)\hat{\mathbf{u}}_i^\dagger(t,0) = \hat{\mathbf{1}}$, we can write the solution of the time-evolution matrix differential equation (3.18) as

$$\hat{\mathbf{u}}_i(t,0) = \begin{bmatrix}\cos(\hat{\omega}_{\rm x1}t) & \sin(\hat{\omega}_{\rm x1}t)\hat{C}\\ -\sin(\hat{\omega}_{\rm x2}t)\hat{C}^\dagger & \cos(\hat{\omega}_{\rm x2}t)\end{bmatrix}, \qquad \text{with} \quad \hat{C} = \frac{\mathrm{i}}{(\hat{B}_-\hat{B}_+)^{1/4}}\sqrt{\hat{B}_-}. \tag{3.20}$$

With this result we can write the final expression for the wavefunction of the system as

$$|\Psi(t)\rangle = \hat{\mathbf{T}}\exp(-\mathrm{i}\hat{\mathbf{h}}_0 t/\hbar)\hat{\mathbf{u}}_i(t,0)|\psi_i(0)\rangle, \tag{3.21}$$

which is valid for any shape-invariant potential coupling a two-level system. As a final remark, we observe that the time-evolution operator $\hat{\mathbf{u}}_i(t,0)$ only contains the operators $\hat{B}_\pm$.

4. The density operator

In discussing two-level systems, we have so far characterized the quantum states in terms of two-component wavefunction $|\Psi(t)\rangle$, presented in (3.12). However, an elegant and very useful way of representing the state of a quantum system is by using the Hermitian density matrix $\hat{\rho}$, defined as

$$\hat{\rho}(t) = \sum_k p_k|\Psi_k(t)\rangle\langle\Psi_k(t)|, \tag{4.1}$$

where p_k is the probability associated with the state $|\Psi_k(t)\rangle$. The normalization condition of $|\Psi(t)\rangle$ requires that $\mathrm{Tr}\,\hat{\rho}(t) = 1$. For a pure state (when all probabilities p_k are zero, except one), a system can be described equally well either by a density operator or by a state vector. However, in the description of a mixed case (a statistical mixture of states), the density matrix formalism presents unquestionable advantages. The time evolution of the density operator is determined by solving the equation of motion $\mathrm{i}\hbar\hat{\rho}' = [\hat{\mathbf{H}}, \hat{\rho}]$, obtained from the definition of the density matrix and the Schrödinger equation. Knowledge of $\hat{\rho}(t)$ enables us to obtain

all other physical quantities since the time evolution of any observable represented with the operator $\hat{O}$ can be obtained by its expectation value evaluated with the density operator of the system

$$\langle \hat{O}(t) \rangle = \frac{\mathrm{Tr}\{\hat{\rho}(t)\hat{O}\}}{\mathrm{Tr}\,\hat{\rho}(t)}. \tag{4.2}$$

To obtain the expectation value of any observable operator it is necessary to calculate the matrix elements of the density operator. To apply the density matrix formalism for the coupled two-level problem we use the state vector given in (3.21) to obtain

$$\hat{\rho}(t) = \hat{\mathbf{T}}\big[\exp(-\mathrm{i}\hat{\mathbf{h}}_0 t/\hbar)\hat{\mathbf{u}}_i(t,0)\hat{\rho}(0)\hat{\mathbf{u}}_i^{\dagger}(t,0)\exp(\mathrm{i}\hat{\mathbf{h}}_0 t/\hbar)\big]\hat{\mathbf{T}}^{\dagger} \tag{4.3}$$

where the initial density operator is given by $\hat{\rho}(0) = |\psi_i(0)\rangle\langle\psi_i(0)|$. Therefore, to get a final expression for the time evolution of the density operator we must define the initial quantum state of the system. We first consider a coherent state, the most *classical* quantum state [27–30]. We assume that the two-level system starts in its lower energy state, i.e.

$$|\psi_i(0)\rangle = \begin{bmatrix} 0 \\ 1 \end{bmatrix} \otimes |z\rangle = \begin{bmatrix} 0 \\ |z\rangle \end{bmatrix} \qquad \text{and} \qquad \hat{\rho}(0) = \frac{1}{2}(\hat{\mathbf{1}} - \hat{\sigma}_3)|z\rangle\langle z|. \tag{4.4}$$

For any analytical function $f(x)$ it is easy to show that $\hat{B}_{\pm} f(\hat{B}_{\mp}\hat{B}_{\pm}) = f(\hat{B}_{\pm}\hat{B}_{\mp})\hat{B}_{\pm}$. Using this property and expression (4.4) for $\hat{\rho}(0)$ it is possible to show that the time-evolved density matrix operator (4.3) can explicitly be expressed as

$$\hat{\rho}(t) = \begin{bmatrix} |\alpha_1(t)\rangle\langle\alpha_1(t)| & |\alpha_1(t)\rangle\langle\alpha_2(t)| \\ |\alpha_2(t)\rangle\langle\alpha_1(t)| & |\alpha_2(t)\rangle\langle\alpha_2(t)| \end{bmatrix} \qquad \text{where} \qquad \begin{cases} |\alpha_1(t)\rangle = \hat{T}\hat{C}\,\mathrm{e}^{-\mathrm{i}\Omega\hat{B}_+\hat{B}_- t}\sin(\hat{\omega}_{x2}t)|z\rangle \\ |\alpha_2(t)\rangle = \mathrm{e}^{-\mathrm{i}\Omega\hat{B}_+\hat{B}_- t}\cos(\hat{\omega}_{x2}t)|z\rangle. \end{cases} \tag{4.5}$$

We next consider the case when the two-level system starts in the state of thermal equilibrium with temperature Θ. We take the initial state as

$$|\psi_i(0)\rangle = \frac{1}{2}[(\hat{\mathbf{1}} + \hat{\sigma}_3)\hat{C} + (\hat{\mathbf{1}} - \hat{\sigma}_3)]\begin{bmatrix} \hat{p}_+ \\ \hat{p}_- \end{bmatrix} \otimes |z\rangle = \begin{bmatrix} \hat{C}\,\hat{p}_+|z\rangle \\ \hat{p}_-|z\rangle \end{bmatrix} \tag{4.6}$$

where

$$\hat{p}_{\pm} = \tfrac{1}{2}[1 \pm \tanh(\beta\hat{\omega}_{x2})] \tag{4.7}$$

with $\beta = \hbar/k_{\mathrm{B}}\Theta$. Thus, the overall coupled system density operator at $t = 0$ can be written as

$$\hat{\rho}(0) = \begin{bmatrix} |\varphi_+\rangle\langle\varphi_+| & |\varphi_+\rangle\langle\varphi_-| \\ |\varphi_-\rangle\langle\varphi_+| & |\varphi_-\rangle\langle\varphi_-| \end{bmatrix} \tag{4.8}$$

where $|\varphi_+\rangle = \hat{C}\,\hat{p}_+|z\rangle$ and $|\varphi_-\rangle = \hat{p}_-|z\rangle$. Using these results it is possible to show that the time-evolved density matrix operator (4.3) still has the same form presented by equation (4.5), but now with the time-dependent states $|\alpha_{1,2}(t)\rangle$ given by

$$\begin{cases} |\alpha_1(t)\rangle = \hat{T}\hat{C}\,\mathrm{e}^{-\mathrm{i}\Omega\hat{B}_+\hat{B}_- t}\{\cos(\hat{\omega}_{x2}t)\,\hat{p}_+ + \sin(\hat{\omega}_{x2}t)\,\hat{p}_-\}|z\rangle \\ |\alpha_2(t)\rangle = \mathrm{e}^{-\mathrm{i}\Omega\hat{B}_+\hat{B}_- t}\{\cos(\hat{\omega}_{x2}t)\,\hat{p}_- - \sin(\hat{\omega}_{x2}t)\,\hat{p}_+\}|z\rangle. \end{cases} \tag{4.9}$$

5. Temporal behaviour of the quantum dynamical variables

5.1. Population inversion factor

For a coupled two-level system an important physical quantity is the population inversion factor [26, 29], defined as

$$\hat{\mathbf{W}} \equiv \hat{\sigma}_+\hat{\sigma}_- - \hat{\sigma}_-\hat{\sigma}_+ = \hat{\sigma}_3. \tag{5.1}$$

The population inversion factor, also called degree of excitation of the system, is typically the simplest nontrivial physical quantity which can be used to analyse the quantum dynamic behaviour of such systems. Inserting the time-evolved density matrix operator (4.3) and the wave state expression (3.21) into equation (4.2) and taking into account the commutation property between $\hat{\mathbf{h}}_0$ and $\hat{\mathbf{T}}$ with $\hat{\sigma}_3$, we obtain

$$\langle\hat{\mathbf{W}}(t)\rangle = \frac{\langle\psi_i(0)|\hat{\rho}(0)\hat{\mathbf{u}}_i(t,0)^\dagger\hat{\sigma}_3\hat{\mathbf{u}}_i(t,0)|\psi_i(0)\rangle}{\langle\psi_i(0)|\hat{\rho}(0)|\psi_i(0)\rangle}. \tag{5.2}$$

Using the operator properties $\hat{C}\hat{\omega}_{\mathrm{x}2} = \hat{\omega}_{\mathrm{x}1}\hat{C}$ and $\hat{C}\hat{C}^\dagger = \hat{C}^\dagger\hat{C} = 1$ and taking into account equation (3.20) for $\hat{\mathbf{u}}_i(t,0)$ we can show that

$$\langle\hat{\mathbf{W}}(t)\rangle = \frac{1}{\langle\psi_i(0)|\psi_i(0)\rangle}\left\{\langle\psi_i(0)\left|\begin{bmatrix}\cos(2\hat{\omega}_{\mathrm{x}1}t) & \sin(2\hat{\omega}_{\mathrm{x}1}t)\hat{C}\\ \sin(2\hat{\omega}_{\mathrm{x}2}t)\hat{C}^\dagger & -\cos(2\hat{\omega}_{\mathrm{x}2}t)\end{bmatrix}\right|\psi_i(0)\rangle\right\}. \tag{5.3}$$

To get an expression for $\langle\hat{\mathbf{W}}(t)\rangle$ we must define the initial state of the system. We assume that the coupled two-level system starts in its pure state (4.4), with the coupling potential coherent state given by equation (2.9), we find the expression

$$\langle\hat{\mathbf{W}}(t)\rangle = -\frac{\langle z;a_r|\cos(2\hat{\omega}_{\mathrm{x}2}t)|z;a_r\rangle}{\langle z;a_r|z;a_r\rangle} \tag{5.4}$$

which, using the series expansion of the cosine function, can be written as

$$\langle\hat{\mathbf{W}}(t)\rangle = -\left[1+\sum_{k=1}^{\infty}\frac{(2\mathrm{i}t)^{2k}}{(2k)!}\frac{\langle z;a_r|\hat{\omega}_{\mathrm{x}2}^{2k}|z;a_r\rangle}{\langle z;a_r|z;a_r\rangle}\right]. \tag{5.5}$$

Using equation (3.19) we conclude that

$$\begin{cases}\langle z;a_r|\hat{\omega}_{\mathrm{u}2}^{2k}|z;a_r\rangle = \lambda^{2k}\langle z;a_r|(\hat{B}_+\hat{B}_- + \Delta^2)^k|z;a_r\rangle, & \text{for} \quad \mathrm{x}=\mathrm{u};\\ \langle z;a_r|\hat{\omega}_{\mathrm{i}2}^{2k}|z;a_r\rangle = \lambda^{2k}\langle z;a_r|[(\hat{B}_+\hat{B}_-)^2 + \Delta^2]^k|z;a_r\rangle, & \text{for} \quad \mathrm{x}=\mathrm{i}.\end{cases} \tag{5.6}$$

To calculate the matrix elements in (5.6) we use expression (2.9) and the commutation between any function of the parameters a_n and the couple of operators $\hat{B}_\pm\hat{B}_\mp$, to show that

$$\langle z;a_r|(\hat{B}_+\hat{B}_- + \Delta^2)^k|z;a_r\rangle/\langle z;a_r|z;a_r\rangle = \sum_{n=0}^{\infty}C_n(e_n+\Delta^2)^k\Bigg/\sum_{n=0}^{\infty}C_n, \quad k\geqslant 1, \tag{5.7}$$

and

$$\langle z;a_r|[(\hat{B}_+\hat{B}_-)^2 + \Delta^2]^k|z;a_r\rangle/\langle z;a_r|z;a_r\rangle = \sum_{n=0}^{\infty}C_n\left(e_n^2+\Delta^2\right)^k\Bigg/\sum_{n=0}^{\infty}C_n, \quad k\geqslant 1, \tag{5.8}$$

where the expansion coefficients are given by $C_0 = 1$ and

$$C_n = \frac{(z^*z)^n}{h_n^*(a_r)h_n(a_r)} = (z^*z)^n\prod_{s=0}^{n-1}\left[\frac{\mathcal{Z}_{j+s}^*\mathcal{Z}_{j+s}}{e_n - e_s}\right], \qquad n\geqslant 1. \tag{5.9}$$

Taking into account the results (5.7) and (5.8) in the matrix elements (5.6) and the series expansion of the cosine function, it is possible to find the following expression for the population inversion factor (5.5),

$$\langle \hat{\mathbf{W}}(t)\rangle = -\sum_{n=0}^{\infty} C_n \cos\left(2\vartheta_n^{(\mathrm{x})}\tau\right) \Bigg/ \sum_{n=0}^{\infty} C_n, \tag{5.10}$$

where $\tau = \lambda t$ is a dimensionless time-associated variable and

$$\vartheta_n^{(\mathrm{u})} = \sqrt{e_n + \Delta^2}, \qquad \text{while} \quad \vartheta_n^{(\mathrm{i})} = \sqrt{e_n^2 + \Delta^2}. \tag{5.11}$$

The sum (5.10) has no known finite analytic expression in the general case. However the physical significance of $\langle \hat{\mathbf{W}}(t)\rangle$ is that it represents, on a scale between -1 and $+1$, the degree of excitation of a two-level system induced by the coupling shape-invariant potential whose quantum state at $t = 0$ is the fully coherent state $|z; a_r\rangle$. In this sense, equation (5.10) can be considered as the generalization for all shape-invariant coupling potentials of the well-known expression originally obtained for two-level atom interacting with radiation [29]. The behaviour of the population inversion factor can be summarized in the following way: if the two-level system is initially in the lower energy state, then the probability for the two-level system to be found in the excited state at the time t regardless of the state of the coupling potential is given by the weighted sum (5.10), which can be rewritten as

$$\langle \hat{\mathbf{W}}(t)\rangle = -\sum_{n=0}^{\infty} P(n, z) \cos\left(2\vartheta_n^{(\mathrm{x})}\tau\right), \tag{5.12}$$

where the weight is given by

$$P(n, z) = C_n \Bigg/ \sum_{n=0}^{\infty} C_n, \tag{5.13}$$

with the weight factor C_n of (5.9). Since each term in the sum (5.10) has a different frequency, as the time increases they become uncorrelated and interfere destructively, causing a collapse in the inversion population factor ($\langle \hat{\mathbf{W}}(t)\rangle \approx 0$). The discrete character of the sum over the quantum states in the coherent state ensures that, after some finite time, all the oscillating terms come back almost in phase with each other, restoring the coherent oscillations and creating periodic revivals in the population inversion factor (periodic packets of finite $\langle \hat{\mathbf{W}}(t)\rangle$ oscillations). However, as the frequencies are not necessarily integers and thus may be incommensurate, the re-phasing is not perfect. Both collapses and revivals in the population inversion factor are purely quantum effects resulting from the discreteness of the coupling potential spectrum and have no classical counterparts. It should be emphasized that the phenomenon of decay and regeneration of the population inversion factor is well known in a few restricted cases, such as quantum optics [29] and a single trapped ion moving in a harmonic potential [31]. Until now, all these known cases of collapse and revival phenomena had been restricted to the harmonic oscillator coupling potential. However, the results found show that the occurrence of this interesting quantum phenomenon is related to the model properties, like the kind of interaction and the coherent-state associated with the coupling potential.

We next consider an initial situation where the coupled two-level system starts in the state (4.6) with $|z\rangle$ given by the coupling potential coherent state $|z; a_r\rangle$. In this case, using the operator properties cited before, we find the following expression:

$$\langle \hat{\mathbf{W}}(t)\rangle = \frac{\langle z; a_r|\left[\hat{p}_+^2 - \hat{p}_-^2\right]\cos(2\hat{\omega}_{\mathrm{x}2}t) + 2\hat{p}_+\hat{p}_- \sin(2\hat{\omega}_{\mathrm{x}2}t)|z; a_r\rangle}{\langle z; a_r|\hat{p}_+^2 + \hat{p}_-^2|z; a_r\rangle}. \tag{5.14}$$

Using the coherent state expression (2.9) for the shape-invariant coupling potential, the series expansions of the exponential and trigonometric functions and the relations (5.6), it is possible to rewrite (5.14) as

$$\langle \hat{\mathbf{W}}(t)\rangle = \sum_{n=0}^{\infty}\left[P_{\mathrm{C}}(n,z,\beta)\cos\left(2\vartheta_n^{(\mathrm{x})}\tau\right) + P_{\mathrm{S}}(n,z,\beta)\sin\left(2\vartheta_n^{(\mathrm{x})}\tau\right)\right], \tag{5.15}$$

where the partial weights are

$$P_{\mathrm{C}}(n,z,\beta) = 2C_n\sqrt{F_n^{(\mathrm{x})}}\Bigg/\sum_{n=0}^{\infty}\left[1+F_n^{(\mathrm{x})}\right]C_n \tag{5.16}$$

$$P_{\mathrm{S}}(n,z,\beta) = \left[1-F_n^{(\mathrm{x})}\right]C_n\Bigg/\sum_{n=0}^{\infty}\left[1+F_n^{(\mathrm{x})}\right]C_n \tag{5.17}$$

with $F_n^{(\mathrm{x})} = \tanh^2\left(\beta\lambda\vartheta_n^{(\mathrm{x})}\right)$. The factors C_n and $\vartheta_n^{(\mathrm{x})}$ are given by (5.9) and (5.11), respectively. Note that if we take the limit $\beta\lambda \to -\infty$ then $\tanh\left(\beta\lambda\vartheta_n^{(\mathrm{x})}\right) \to -1$ and we reproduce the result obtained for the pure state case, characterized by $\hat{p}_- \to 1$ and $\hat{p}_+ \to 0$.

5.2. *Intensity of the shape-invariant coupling*

If we define the quantity $\hat{\mathbf{N}}_{\mathrm{B}} = \frac{1}{2}[\hat{\mathbf{1}} - \hat{\sigma}_3]\hat{B}_+\hat{B}_-$, then its expectation value allows us to understand the global influence of the coupling. This definition represents a generalization of the excitation number $\hat{N}$ used in quantum optics. If we insert the time-evolved density matrix operator (4.3) and the wave state expression (3.21) into equation (4.2) and take into account the commutation property between $\hat{\mathbf{h}}_0$ and $\hat{\mathbf{T}}$ with $\hat{\sigma}_3$, we obtain

$$\langle \hat{\mathbf{N}}_{\mathrm{B}}(t)\rangle = \frac{\langle\psi_i(0)|\hat{\rho}(0)\hat{\mathbf{u}}_i(t,0)^{\dagger}\hat{\mathbf{N}}_{\mathrm{B}}\hat{\mathbf{u}}_i(t,0)|\psi_i(0)\rangle}{\langle\psi_i(0)|\hat{\rho}(0)|\psi_i(0)\rangle}. \tag{5.18}$$

Using the operator properties $\hat{C}\hat{\omega}_{\mathrm{x}2} = \hat{\omega}_{\mathrm{x}1}\hat{C}$ and $\hat{C}\hat{C}^{\dagger} = \hat{C}^{\dagger}\hat{C} = 1$ and taking into account equation (3.20) for $\hat{\mathbf{u}}_i(t,0)$ we can show that

$$\langle \hat{\mathbf{N}}_{\mathrm{B}}(t)\rangle = \frac{1}{\langle\psi_i(0)|\psi_i(0)\rangle} \times\left\{\langle\psi_i(0)\left|\begin{bmatrix}\hat{B}_-\hat{B}_+\sin^2(\hat{\omega}_{\mathrm{x}1}t) & -\frac{1}{2}\hat{B}_-\hat{B}_+\sin(2\hat{\omega}_{\mathrm{x}1}t)\hat{C}\\ -\frac{1}{2}\hat{B}_+\hat{B}_-\sin(2\hat{\omega}_{\mathrm{x}2}t)\hat{C}^{\dagger} & \hat{B}_+\hat{B}_-\cos^2(\hat{\omega}_{\mathrm{x}2}t)\end{bmatrix}\right|\psi_i(0)\rangle\right\}. \tag{5.19}$$

To find an expression for $\langle \hat{\mathbf{N}}_{\mathrm{B}}(t)\rangle$ we must define the initial state of the system. If we assume that the coupled two-level system starts in the pure state of (4.4), with the coupling potential coherent state given by equation (2.9), we find the expression

$$\langle \hat{\mathbf{N}}_{\mathrm{B}}(t)\rangle = \frac{\langle z;a_r|\hat{B}_+\hat{B}_-\cos^2(\hat{\omega}_{\mathrm{x}2}t)|z;a_r\rangle}{\langle z;a_r|z;a_r\rangle} \tag{5.20}$$

which, using the series expansion of the cosine function, can be written as

$$\langle \hat{\mathbf{N}}_{\mathrm{B}}(t)\rangle = \sum_{n=0}^{\infty}P(n,z)e_n\cos^2\left(\vartheta_n^{(\mathrm{x})}\tau\right). \tag{5.21}$$

If we assume the system instead starts in the state (4.6) where the state $|z\rangle$ is given by $|z; a_r\rangle$, we find the following expression,

$$\langle \hat{\mathbf{N}}_{\mathrm{B}}(t)\rangle = \frac{\langle z; a_r|\hat{B}_+\hat{B}_-\{[\hat{p}_+^2+\hat{p}_-^2]-[\hat{p}_+^2-\hat{p}_-^2]\cos(2\hat{\omega}_{\mathrm{x}2}t)-2\hat{p}_+\hat{p}_-\sin(2\hat{\omega}_{\mathrm{x}2}t)\}|z; a_r\rangle}{2\langle z; a_r|\hat{p}_+^2+\hat{p}_-^2|z; a_r\rangle} \tag{5.22}$$

which, with the series expansion of the cosine function, can be written as

$$\langle \hat{\mathbf{N}}_{\mathrm{B}}(t)\rangle = \frac{1}{2}\sum_{n=0}^{\infty}\left[P_{\mathrm{O}}(n,z,\beta)-P_{\mathrm{C}}(n,z,\beta)\cos\left(2\vartheta_n^{(\mathrm{x})}\tau\right)-P_{\mathrm{S}}(n,z,\beta)\sin\left(2\vartheta_n^{(\mathrm{x})}\tau\right)\right]e_n, \tag{5.23}$$

where the partial weights $P_{\mathrm{C}}(n,z,\beta)$ and $P_{\mathrm{S}}(n,z,\beta)$ are still given by equations (5.16) and (5.17), while

$$P_{\mathrm{O}}(n,z,\beta) = \left[1+F_n^{(\mathrm{x})}\right]C_n \Bigg/ \sum_{n=0}^{\infty}\left[1+F_n^{(\mathrm{x})}\right]C_n. \tag{5.24}$$

5.3. Mandel parameter for the distribution deviations

The final dynamical variable we wish to study is the generalization of the Mandel parameter defined as

$$Q_{\mathrm{M}}(t) = \frac{[\Delta\hat{\mathbf{N}}_{\mathrm{B}}(t)]^2-\langle\hat{\mathbf{N}}_{\mathrm{B}}(t)\rangle}{\langle\hat{\mathbf{N}}_{\mathrm{B}}(t)\rangle}, \qquad \text{where} \quad [\Delta\hat{\mathbf{N}}_{\mathrm{B}}(t)]^2 = \left\langle\hat{\mathbf{N}}_{\mathrm{B}}^2(t)\right\rangle - \langle\hat{\mathbf{N}}_{\mathrm{B}}(t)\rangle^2 \tag{5.25}$$

which measures the deviation from the regular coherent state quantum states distribution $P(n,z)$. Using the properties of the $\hat{B}$ operators presented in the first section and the coherent state definition (2.8) it is easy to verify that the Mandel parameter assumes the values -1 for the pure coupling potential quantum state $|n\rangle$ and the critical coherent value

$$Q_{\mathrm{ch}} = |z|^2[|\mathcal{Z}_{j-2}|^2-|\mathcal{Z}_{j-1}|^2]+R_1-1 \tag{5.26}$$

for the pure coupling potential generalized coherent state $|z; a_r\rangle$. The critical value separates the *sub-coherent* distribution, defined when $Q_{\mathrm{M}}(t) < Q_{\mathrm{ch}}$, from the *super-coherent* distribution defined when $Q_{\mathrm{M}}(t) > Q_{\mathrm{ch}}$. As we will see in the applications of the next section, for a harmonic oscillator coupling potential $Q_{\mathrm{ch}} = 0$ and the regular distribution $P(n,z)$ is Poissonian.

It is straightforward to show that the Mandel parameter reads

$$Q_{\mathrm{M}}(t) = \frac{\sum_{n=0}^{\infty}P(n,z)e_n^2\cos^2\left(\vartheta_n^{(\mathrm{x})}\tau\right)}{\sum_{n=0}^{\infty}P(n,z)e_n\cos^2\left(\vartheta_n^{(\mathrm{x})}\tau\right)} - \sum_{n=0}^{\infty}P(n,z)e_n\cos^2\left(\vartheta_n^{(\mathrm{x})}\tau\right)-1 \tag{5.27}$$

for the initial pure state (4.4), and

$$\begin{aligned} Q_{\mathrm{M}}(t) = {} & \frac{\sum_{n=0}^{\infty}\left[P_{\mathrm{O}}(n,z,\beta)-P_{\mathrm{C}}(n,z,\beta)\cos\left(2\vartheta_n^{(\mathrm{x})}\tau\right)-P_{\mathrm{S}}(n,z,\beta)\sin\left(2\vartheta_n^{(\mathrm{x})}\tau\right)\right]e_n^2}{\sum_{n=0}^{\infty}\left[P_{\mathrm{O}}(n,z,\beta)-P_{\mathrm{C}}(n,z,\beta)\cos\left(2\vartheta_n^{(\mathrm{x})}\tau\right)-P_{\mathrm{S}}(n,z,\beta)\sin\left(2\vartheta_n^{(\mathrm{x})}\tau\right)\right]e_n} \\ & -\frac{1}{2}\sum_{n=0}^{\infty}\left[P_{\mathrm{O}}(n,z,\beta)-P_{\mathrm{C}}(n,z,\beta)\cos\left(2\vartheta_n^{(\mathrm{x})}\tau\right)-P_{\mathrm{S}}(n,z,\beta)\sin\left(2\vartheta_n^{(\mathrm{x})}\tau\right)\right]e_n-1 \end{aligned} \tag{5.28}$$

for the initial mixed state (4.6).

6. Applications for some shape-invariant coupling potentials

In order to investigate how our general results can be applied in specific cases in this section we consider three examples of the shape-invariant coupling potentials: the harmonic oscillator, the Pöschl–Teller and the self-similar potentials. It should be noted that the expressions obtained for the quantum dynamical variables of the system are general and applicable for all shape-invariant coupling potentials. Applying the general approach for a given shape-invariant coupling potential we need to specify only the energy spectrum e_n and the coherent state form defined by the expansion coefficient $h_n(a_r)$. Using these factors we obtain the function argument $\vartheta_n^{(\mathrm{x})}$ and the expansion coefficients C_n. Therefore in these applications all we need is to specify e_n and $h_n(a_r)$. The numerical evaluation of series is a nontrivial problem; we used the Smith [32] routines package of multiple precision computation.

6.1. Harmonic oscillator potential

We start with this example because it is the simplest among the shape-invariant coupling potentials. We would also like to show that our general expressions reduce to the well-known expressions for the harmonic oscillator. The partner potentials (1.3) for this system are obtained with the superpotential

$$W(x, a_1) = \sqrt{\hbar\Omega}(\varrho x + \delta), \tag{6.1}$$

where ϱ and δ are real constants, and $R(a_n) = \eta(a_n + a_{n+1})$, $\eta = \sqrt{\hbar/(2m\Omega)}$. Since the parameters for this potential are related by $a_1 = a_2 = \cdots = a_n = \varrho$ we get $R(a_n) = \gamma$, with $\gamma = 2\eta\varrho$, and thus

$$e_n = n\gamma. \tag{6.2}$$

The constant values of the potential parameters a_n imply that for this system we must have $\mathcal{Z}_j = c$, a constant. Under these conditions equation (2.10) gives us $h_n(a_r) = \sqrt{\gamma^n n!}/c^n$. If we redefine the complex constant by $z \longrightarrow cz/\sqrt{\gamma}$, and take into account that $|n\rangle$ is an element of the Fock space $\mathcal{F} \equiv \{|n\rangle, n \geqslant 0\}$, we find for the coherent state (2.9)

$$|z; a_r\rangle = \sum_{n=0}^{\infty} \frac{z^n}{\sqrt{n!}}|n\rangle \tag{6.3}$$

which is the usual expression for bosonic coherent states [23]. The expansion coefficient C_n and the function argument factors $\vartheta_n^{(\mathrm{x})}$ are given by

$$C_n = \frac{|z|^{2n}}{n!}, \qquad \text{with} \quad \vartheta_n^{(\mathrm{u})} = \sqrt{\gamma n + \Delta^2} \qquad \text{and} \qquad \vartheta_n^{(\mathrm{i})} = \sqrt{(\gamma n)^2 + \Delta^2}. \tag{6.4}$$

With the expressions for C_n and $\vartheta_n^{(\mathrm{x})}$ obtained we are ready to get the expressions for the quantum dynamical variables. In this case the weight function $P(n, z)$ is given by

$$P(n, z) = \left(\frac{|z|^{2n}}{n!}\right) \mathrm{e}^{-|z|^2}, \tag{6.5}$$

which corresponds to a Poisson distribution centred at $|z|^2$ with width $|z|$. Note that if we use (6.5) and the series expression for the exponential function into (5.12) in the case of pure initial state (4.4) we get the well-known expression for the population inversion factor for a two-level atom interacting with radiation [29].

Figure 1 displays the quantum dynamical variables for the constant (x = u) interaction case in terms of the time variable τ/π, when the initial state of the system is the pure quantum state (4.4). In these calculations we used $|z|^2 = 40$, $\gamma = 1$ and $\Delta = 0.2$. It should be noted

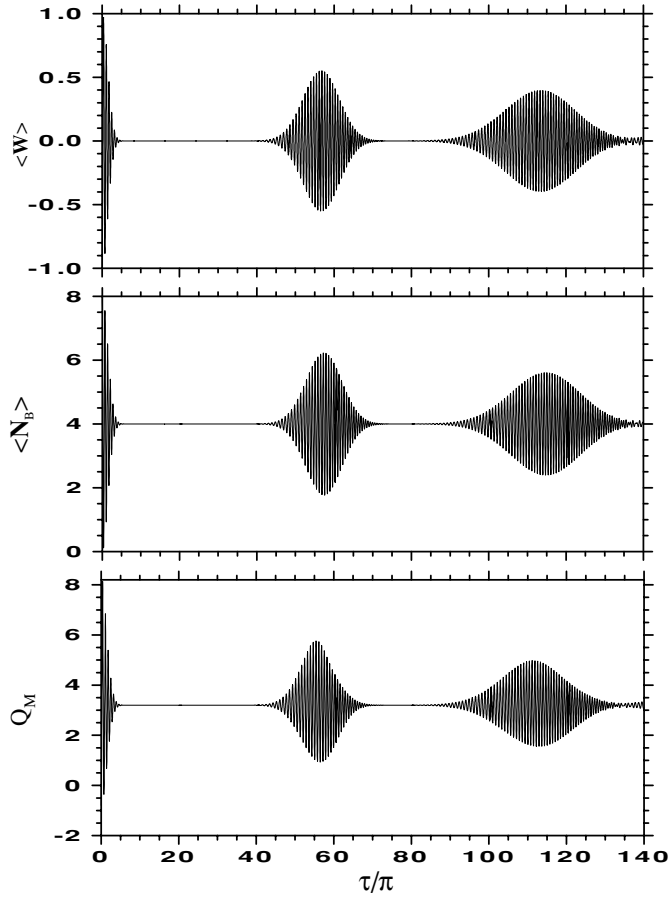

Figure 1. Time evolution of the dynamical variables for a harmonic oscillator coupling potential in the constant interaction case (x = u) for a pure initial state. The constant values used are $|z|^2 = 40$, $\gamma = 1$ and $\Delta = 0.2$.

that in general the dynamical variables $\langle\hat{\mathbf{W}}(t)\rangle$, $\langle\hat{\mathbf{N}}_{\mathrm{B}}(t)\rangle$ and $Q_{\mathrm{M}}(t)$ show Rabi oscillations with a period $\tau_{\mathrm{O}} \approx 2\pi/\vartheta_{\bar{n}}^{(\mathrm{u})} \approx 0.7\pi$, where $\bar{n} = |z|^2$. These oscillations collapse with a *collapse time* $\tau_{\mathrm{C}} \approx \sqrt{\bar{n}}\pi \approx 6.3\pi$, and the revivals, bounded by monotonically decreasing Gaussian envelopes, recur periodically (*revival time* $\tau_{\mathrm{R}} \approx \bar{n}\pi = 40\pi$), become less complete and broaden, eventually overlapping with each other at still longer times. Besides this general behaviour, we note a little deformation in the envelope of $Q_{\mathrm{M}}(t)$ when we compare its bottom and top parts. The critical coherent value of the Mandel parameter in this case is $Q_{\mathrm{ch}} = 0$. Therefore, we conclude that during the time evolution the coupling potential quantum states distribution involved in the total system state remains super-coherent ($Q_{\mathrm{M}}(t) > Q_{\mathrm{ch}}$) almost all the time. Only during a short time interval at the beginning this is not the case.

Figure 2 is the same as figure 1 but for the mixed initial quantum state of the system (4.6) with $\beta\lambda = \hbar\lambda/(k_{\mathrm{B}}\Theta) = 1$. The values of the other constants used in these calculations are the same as that in figure 1. In general, the behaviour of the dynamical variables $\langle\hat{\mathbf{W}}(t)\rangle$, $\langle\hat{\mathbf{N}}_{\mathrm{B}}(t)\rangle$ and $Q_{\mathrm{M}}(t)$ is the same as in the previous case, showing collapses and revivals with almost the same characteristic times, but with different initial conditions. However in this case the

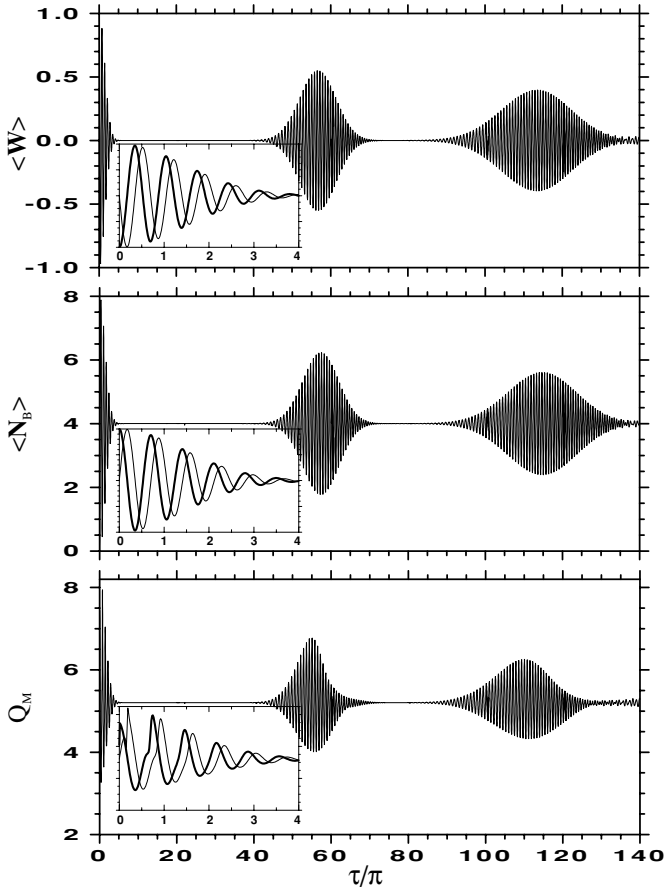

Figure 2. Same as figure 1 calculated with the same strengths but for a mixed initial state of the system with $\beta\lambda = 1$. The insets display magnified views in time of the first collapse event for two different temperature values: $\beta\lambda = 1$ (thick line) and $\beta\lambda = 0$ (thin line).

deformation observed in the envelope of $Q_{\mathrm{M}}(t)$ is more evident. In addition, the system quantum state is super-coherent during the time evolution. In order to get an idea about the temperature effects on the results we show in the insets in this figure magnified views in time of the first collapse event for two different temperature values. The thick line is obtained for $\beta\lambda = 1$ while the thin line for $\beta\lambda = 0$. If we compare the two calculations we observe that the net effect of the temperature on the quantum dynamical variables is a translation in time, preserving its profile.

Figures 3 and 4 are the versions of figures 1 and 2, respectively, for the intensity-dependent interaction (x = i) calculated with the same set of parameters. Note that, when the interaction is intensity-dependent, the Rabi oscillations of the quantum dynamical variables have a period $\tau_{\mathrm{O}} \approx 1/\vartheta_{\bar{n}}^{(\mathrm{i})} \approx 0.25\pi$ and the oscillations collapse after a *collapse time* $\tau_{\mathrm{C}} \approx \sqrt{\bar{n}}/2 \approx \pi$. The revival events have Gaussian envelopes and are almost exact regeneration of the initial oscillations with a *revival period* $\tau_{\mathrm{R}} \approx \bar{n}\pi/4 = 10\pi$. Indeed, as shown in [26], exact regeneration happens when the system is resonant ($\Delta = 0$). These and other properties for the inversion population factor and its relation with the system parameters in the case of the harmonic oscillator coupling potential for the constant and intensity-dependent interaction

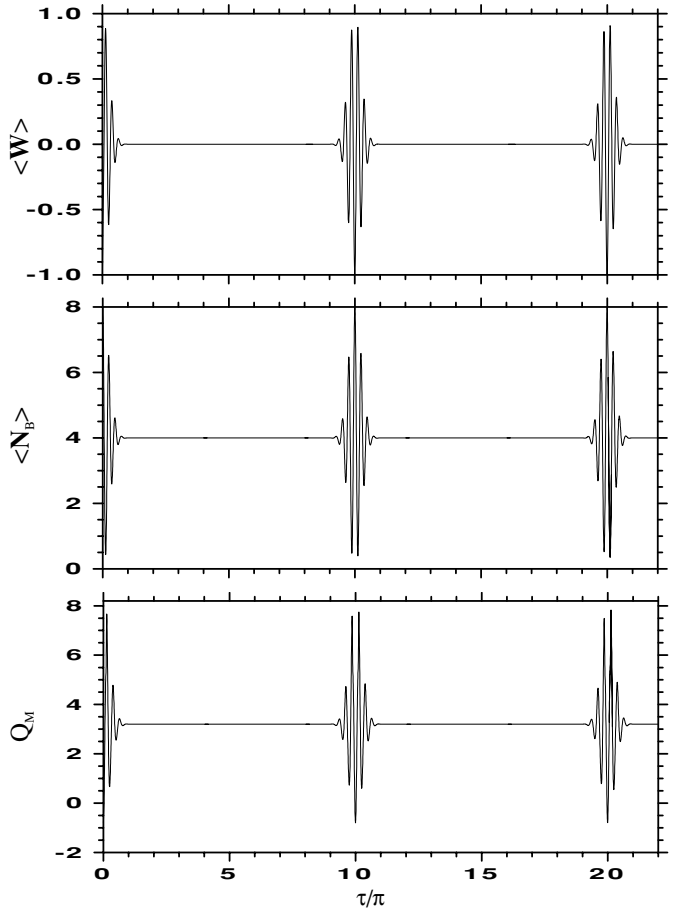

Figure 3. Same as figure 1, but for the intensity-dependent interaction case (x = i).

cases are exhaustively analysed and discussed in [26, 29] when we have a pure initial quantum state.

It should be pointed out that in the case of a mixed initial state (4.6) for the intensity-dependent (x = i) interaction the deformation observed in the envelope of $Q_{\mathrm{M}}(t)$ is more apparent than other cases, showing the asymmetry between the top and the bottom parts of the envelopes. On the other hand, looking at the insets in the figures showing magnified views in time, for the first collapse event with two different temperature values ($\beta\lambda = 1$ and 0) we conclude that the effect is not only a translation in time of the curve, but also a deformation during the revival events. To conclude this discussion about the behaviour of the dynamical variables for the harmonic oscillator coupling potential case we can say that the inversion population factor $\langle\hat{\mathbf{W}}(t)\rangle$, the intensity of the shape-invariant coupling $\langle\hat{\mathbf{N}}_{\mathrm{B}}(t)\rangle$ and the Mandel parameter $Q_{\mathrm{M}}(t)$ exhibit similar time evolutions, with equal characteristic time factors (Rabi's period, collapse times and revival period). In the case of $\langle\hat{\mathbf{W}}(t)\rangle$ and $\langle\hat{\mathbf{N}}_{\mathrm{B}}(t)\rangle$ it is easy to understand this similarity since we have

$$\langle\hat{\mathbf{N}}_{\mathrm{B}}(t)\rangle = \frac{\gamma|z|^2}{2}[1 - \langle\hat{\mathbf{W}}(t)\rangle]. \tag{6.6}$$

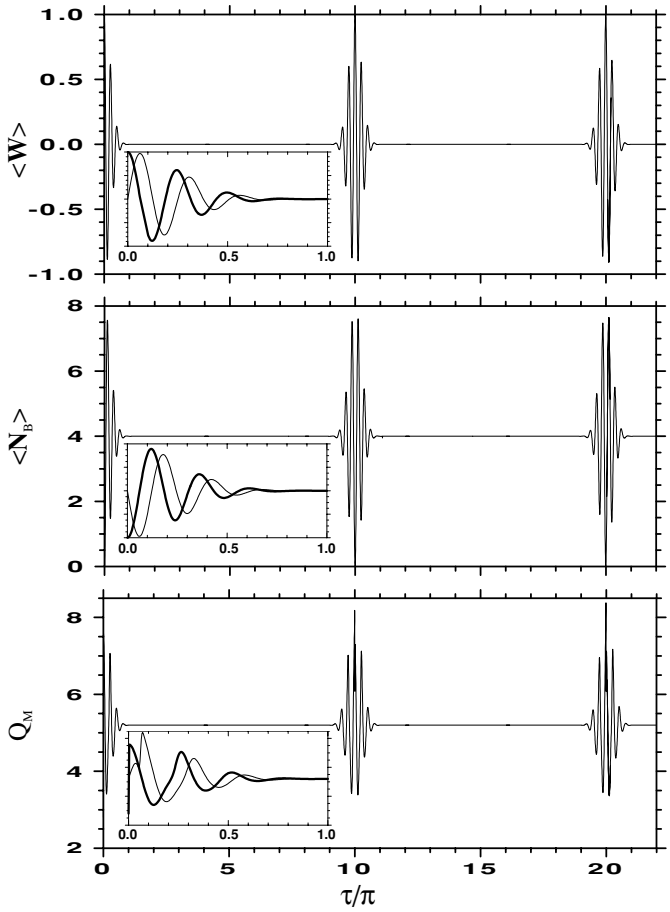

Figure 4. Same as figure 2, but for the intensity-dependent interaction case (x = i).

The Mandel parameter $Q_{\mathrm{M}}(t)$ has almost the same characteristic time factors because it is defined by the energy spectrum e_n of the coupling potential.

6.2. Pöschl–Teller potential

The Pöschl–Teller potential, originally introduced in a molecular physics context, is closely related to several other potentials, widely used in molecular and solid state physics such as, for example, the Scarf potential, used in the modelling of 1D crystal, and the Rosen–Morse potential, used in molecular models. In addition, the Pöschl–Teller potential becomes the infinite square well in a limiting case. The superpotential, related to the Pöschl–Teller potential via equation (1.3), is given by [33]

$$W(x, a_1) = \sqrt{\hbar\Omega}\{\varrho(a_1 + \gamma)\cot[\varrho(x + \lambda)] + \delta\csc[\varrho(x + \lambda)]\}, \tag{6.7}$$

where ϱ, γ, δ and λ are real constants, while the remainders [1] in the shape-invariant condition (2.1) are given by $R(a_n) = \varrho^2\eta[2(a_n + \gamma) + \eta]$, with the potential parameters related by $a_{n+1} = a_n + \eta$, where $\eta = \sqrt{\hbar/(2m\Omega)}$. Inserting these results into (2.6) we can prove that

$$e_n = \kappa^2 n(n + 2\sigma), \tag{6.8}$$

with $\kappa = \varrho\eta$ and $\sigma = (a_1 + \gamma)/\eta$. To obtain the coherent state of the Pöschl–Teller potential, we define the functional $\mathcal{Z}_j$

$$\mathcal{Z}_j = \sqrt{g(a_1; 2\kappa/\eta, \kappa)g(a_1; 2\kappa/\eta, 2\kappa)}\, \mathrm{e}^{-\mathrm{i}\alpha R(a_1)} \tag{6.9}$$

where the auxiliary function is given by $g(a_j; c, d) = ca_j + d$ and α is a real constant. It follows that

$$\prod_{k=0}^{n-1} \mathcal{Z}_{j+k} = \sqrt{\frac{\kappa^{2n}\Gamma(\nu + 2n + 1)}{\Gamma(\nu + 1)}}\, \mathrm{e}^{-\mathrm{i}\alpha e_n} \tag{6.10}$$

with $\nu = 2a_1/\eta$. Assuming $\gamma = \eta/2$ and using (6.8) and (6.10) into (2.10) and (2.9) we find that

$$\begin{aligned} h_n(a_r) &= \sqrt{\frac{\Gamma(\nu + 1)\Gamma(n + 1)}{\Gamma(\nu + n + 1)}}\, \mathrm{e}^{\mathrm{i}\alpha e_n}, \\ |z; a_r\rangle &= \sum_{n=0}^{\infty} \sqrt{\frac{\Gamma(\nu + n + 1)}{\Gamma(\nu + 1)\Gamma(n + 1)}}\, \mathrm{e}^{-\mathrm{i}\alpha e_n} z^n |n\rangle. \end{aligned} \tag{6.11}$$

The expansion coefficients C_n and the function argument factors $\vartheta_n^{(\mathrm{x})}$ are given by

$$\begin{aligned} C_n = \frac{|z|^{2n}\Gamma(\nu + n + 1)}{\Gamma(\nu + 1)\Gamma(n + 1)}, \qquad \vartheta_n^{(\mathrm{u})} = \sqrt{\kappa^2 n(n + \nu + 1) + \Delta^2}, \qquad \text{and} \\ \vartheta_n^{(\mathrm{i})} = \sqrt{[\kappa^2 n(n + \nu + 1)]^2 + \Delta^2}. \end{aligned} \tag{6.12}$$

For the pure initial state (4.4) we can use (6.12) and the identity

$$\frac{1}{\Gamma(\nu + 1)} \sum_{n=0}^{\infty} \frac{\Gamma(\nu + n + 1)}{\Gamma(n + 1)} |z|^{2n} = (1 - |z|^2)^{-(\nu+1)}, \tag{6.13}$$

valid when $|z| < 1$, in (5.12) and obtain an expression for the weight distribution function:

$$P(n, z) = \frac{(1 - |z|^2)^{\nu+1}}{\Gamma(\nu + 1)} \left[\frac{\Gamma(\nu + n + 1)}{\Gamma(n + 1)}\right] |z|^{2n}. \tag{6.14}$$

Figure 5 shows the results for the quantum dynamical variables for the constant (x = u) interaction case in terms of the time variable τ/π, when the initial state of the system is the pure quantum state (4.4). In these calculations we used the values $|z|^2 = 0.75$, $\kappa^2 = 0.2$, $\nu = 5.5$ and $\Delta = 0.2$. In this case the dynamical variables $\langle\hat{\mathbf{W}}(t)\rangle$, $\langle\hat{\mathbf{N}}_{\mathrm{B}}(t)\rangle$ and $Q_{\mathrm{M}}(t)$ show Rabi oscillations compressed in time inside each revival event. Therefore it is not possible to define a period for it. These revivals are bounded by asymmetric envelopes that recur periodically with the *revival time* $\tau_{\mathrm{R}} \approx 10\pi$ and show more oscillations after each event. During the revival event the oscillations collapse abruptly with *collapse time* rising because of the increase in the oscillation number in each subsequent revival event. On the other hand, this increase in the oscillation number makes the revivals overlap with each other later and the result is an irregular and quasi-chaotic curve. If we compare the results for the three dynamical variables studied it is possible to verify that the inversion population factor $\langle\hat{\mathbf{W}}(t)\rangle$ shows larger oscillations in time than the other two variables. It is also evident from the figure that the asymmetry of the Mandel factor $Q_{\mathrm{M}}(t)$ in relation to the collapse base line is more noticeable in this case. The critical coherent value of the Mandel parameter is found to be

$$Q_{\mathrm{ch}} = \kappa^2\{2|z|^2(3 - 2\nu) + \nu + 2\} - 1 \tag{6.15}$$

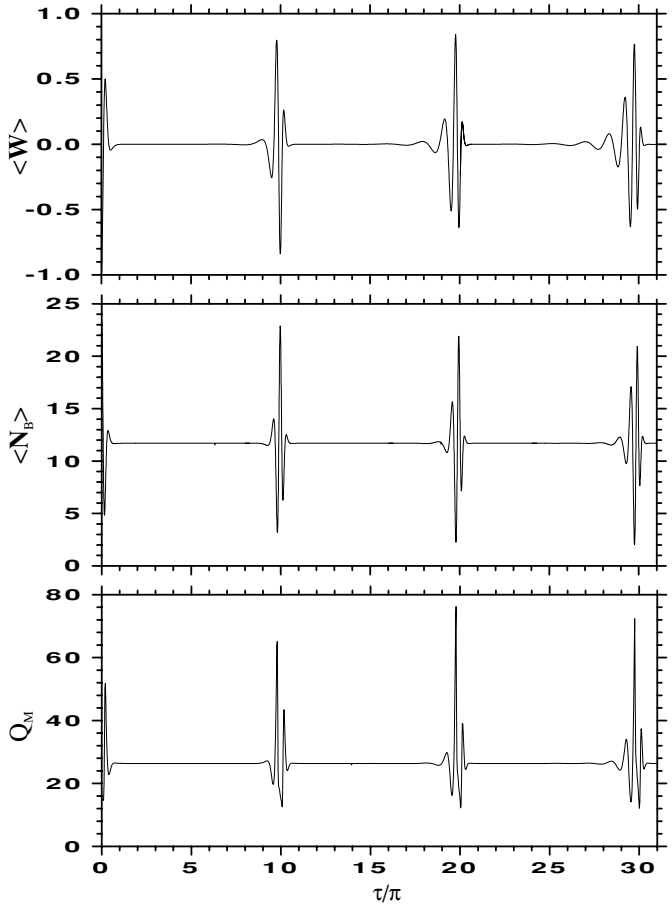

Figure 5. Time evolution of the dynamical variables for a Pöschl–Teller coupling potential in the constant interaction case (x = u) for a pure initial state. The constant values used are $|z|^2 = 0.75$, $\kappa^2 = 0.2$, $\nu = 5.5$ and $\Delta = 0.2$.

that, in the case of the constants used in this figure, gives the numerical value $Q_{\rm ch} = -1.9$. As $Q_{\rm M}(t) > Q_{\rm ch}$ all the time we conclude that the coupling potential quantum states distribution is always super-coherent.

Figure 6 is the version of figure 5 for the mixed initial quantum state (4.6) with $\beta\lambda = \hbar\lambda/(k_{\rm B}\Theta) = 1$. The values of the other parameters are the same as that in figure 1. In general, the behaviour of the three dynamical variables is the same as in the case of the pure initial quantum state of the system, showing collapses and revivals with almost the same characteristic times, but with different initial conditions. However, $Q_{\rm M}(t)$ in this case presents a more complicated pattern originating from the overlapping of different kinds of oscillations. In order to have a more clear view of this new behaviour and to get an idea about the temperature effects on the results, we show in the insets in this figure magnified views in time of the first complete revival event for two different temperature values. The thick and the thin lines were obtained for $\beta\lambda = 1$ and $\beta\lambda = 0$, respectively. We observe that the net effect of the temperature on the quantum dynamical variables is not only a shift in time of the curve, but also a change in its profile because of the superposition effects referred to above.

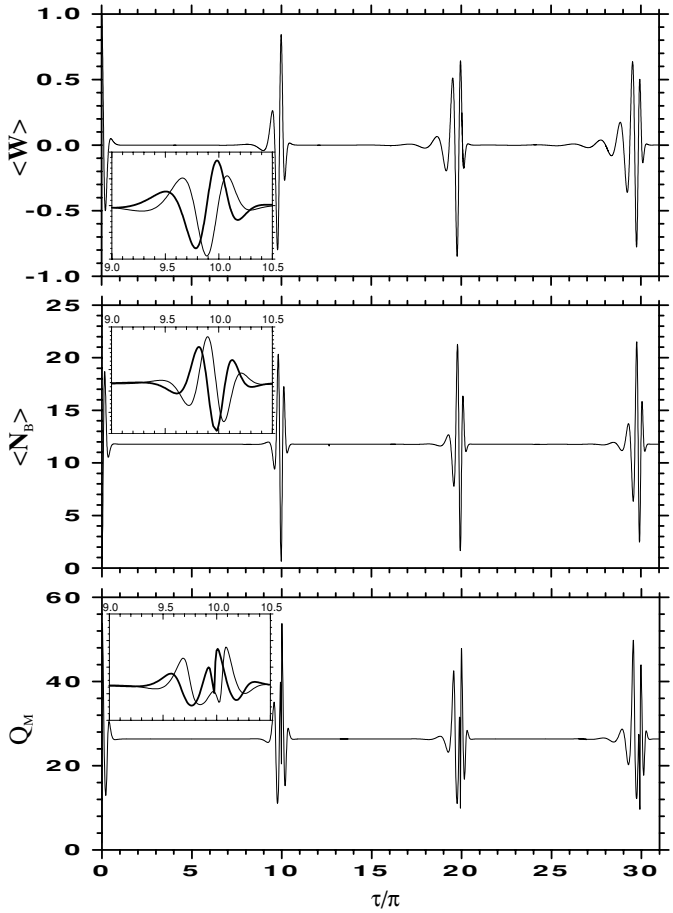

Figure 6. Same as figure 5; calculated with the same strengths but for a mixed initial state of the system with $\beta\lambda = 1$. The insets display magnified views in time of the first revival event for two different temperature values: $\beta\lambda = 1$ (thick line) and $\beta\lambda = 0$ (thin line).

We also note the super-coherent character of the system quantum state during all the time of its evolution ($Q_{\mathrm{M}}(t) > Q_{\mathrm{ch}}$).

Figures 7 and 8 are the versions of figures 5 and 6, respectively, for the intensity-dependent interaction (x = i) calculated with $|z|^2 = 0.60$, $\kappa^2 = 0.02$, $\nu = 14.5$ and $\Delta = 0.2$. The calculations for the mixed initial quantum state of the system, shown in figure 8, were done with the same temperature factors used in figure 6. Note that, in the intensity-dependent interaction case, the Rabi oscillations of the quantum dynamical variables present a regular pattern with a defined period inside each revival event. The revival envelopes show a symmetric form and each oscillation packet has its own pattern and oscillation period. Again, as in the previous cases, the deviations from the main features of the dynamical behaviour appear in the Mandel factor $Q_{\mathrm{M}}(t)$, which now shows an additional revival event around $\tau \approx 50\pi$ with a short oscillation period. The net effect of a finite temperature on the quantum dynamical variables is a shift in time supplemented by a shift-up in the base line of the curve, while preserving its pattern. The super-coherent character of the system quantum state during its evolution is still also present.

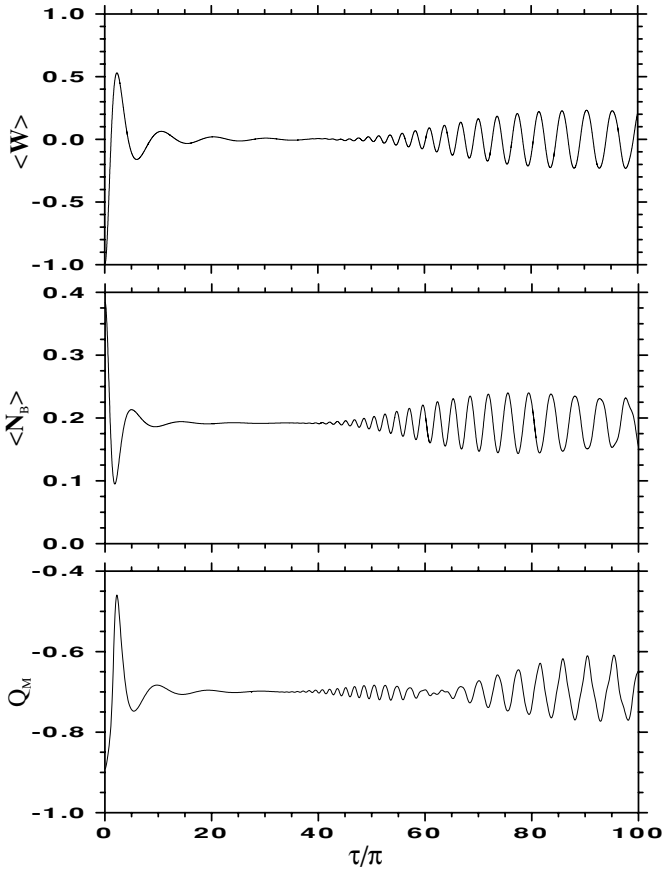

Figure 7. Same as figure 5, but for the intensity-dependent interaction case (x = i) calculated with the constant values $|z|^2 = 0.6$, $\kappa^2 = 0.02$, $\nu = 14.5$ and $\Delta = 0.2$.

The set of system parameters used to get our results for the Pöschl–Teller coupling potential was chosen to make evident the collapse and revival phenomenon in the physical quantities. The collapse and revival times depend mainly on the values of the ν and κ parameters. The detuning Δ parameter basically defines the temporal position of the whole oscillatory pattern, without distortions. Finally, the role of the $|z|^2$ parameter is mainly related to the oscillatory pattern amplitude. We avoided including figures showing this fact because too many figures are already included in the paper.

One can now contrast the Pöschl–Teller coupling potential with the harmonic oscillator. The collapses and revivals are still present, as in the harmonic oscillator coupling case, but with some new and very interesting properties, such as undefined Rabi oscillation periods, revivals with asymmetric envelopes and increases in the Rabi oscillations. All these properties are related to the form of new kind of coupling potential, introduced by the presence of its eigenvalues e_n in the arguments of time-dependent expressions for the dynamical variables.

As a final observation about these applications we must point out that the possible left–right symmetry of the Pöschl–Teller coupling potential, characterized by the value of the δ parameter, does not have influence on the results shown in the figures. This parameter influences the shape of the Pöschl–Teller potential, however has no effect on its energy

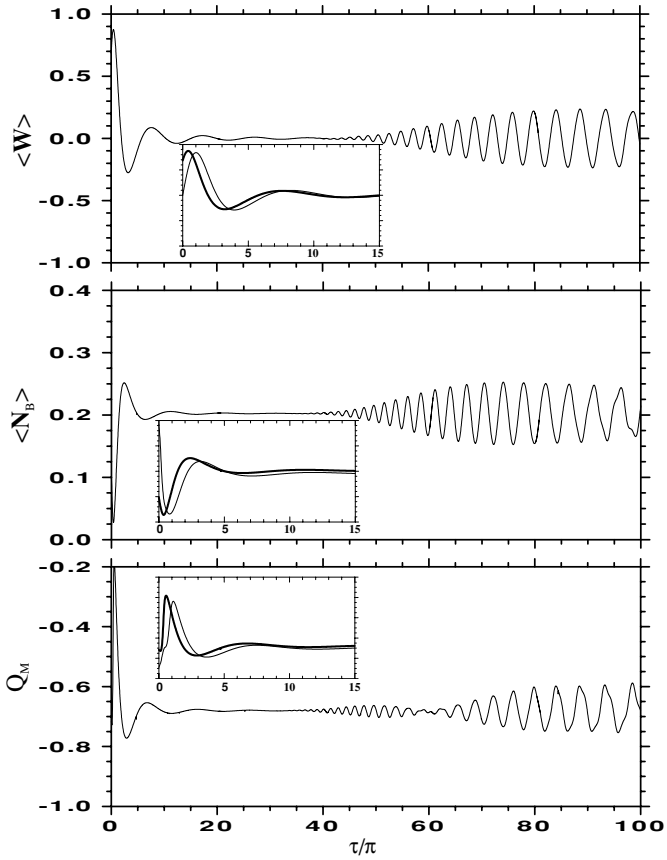

Figure 8. Same as figure 6, but for the intensity-dependent interaction case (x = i) calculated with the constant values $|z|^2 = 0.6$, $\kappa^2 = 0.02$, $\nu = 14.5$ and $\Delta = 0.2$.

spectrum e_n and on the potential parameters a_n. Since our general approach requires to specify only the energy spectrum e_n and the arbitrary functional $\mathcal{Z}_j \equiv \mathcal{Z}(a_1, a_2, a_3, \ldots)$ of the potential parameters to get the expansion coefficients C_n, the results do not have sensitivity on this symmetry.

6.3. Self-similar potential

So far we have considered examples where the parameters a_n of the partner potentials $V_\pm(x)$ are related by a translation. One class of shape-invariant potentials is given by an infinite chain of reflectionless potentials $V_\pm^{(k)}(x)$, $(k = 0, 1, 2, \ldots)$, for which associated superpotentials $W_k(x)$ satisfy the self-similar *ansatz* $W_k(x) = q^k W(q^k x)$, with $0 < q < 1$. These sets of partner potentials $V_\pm^{(k)}(x)$, also called self-similar potentials [34], have an infinite number of bound states and its parameters are related by a scaling: $a_n = q^{n-1}a_1$, $\forall n \in \mathbb{Z}$. These self-similar potentials can be considered as quantum deformations of the multisoliton solutions corresponding to the Rosen–Morse potential. Indeed working with this kind of potential it is possible to get the Rosen–Morse, harmonic oscillator and Pöschl–Teller potentials as limiting cases [34]. Shape invariance of self-similar potentials was studied in detail in [22]. In the

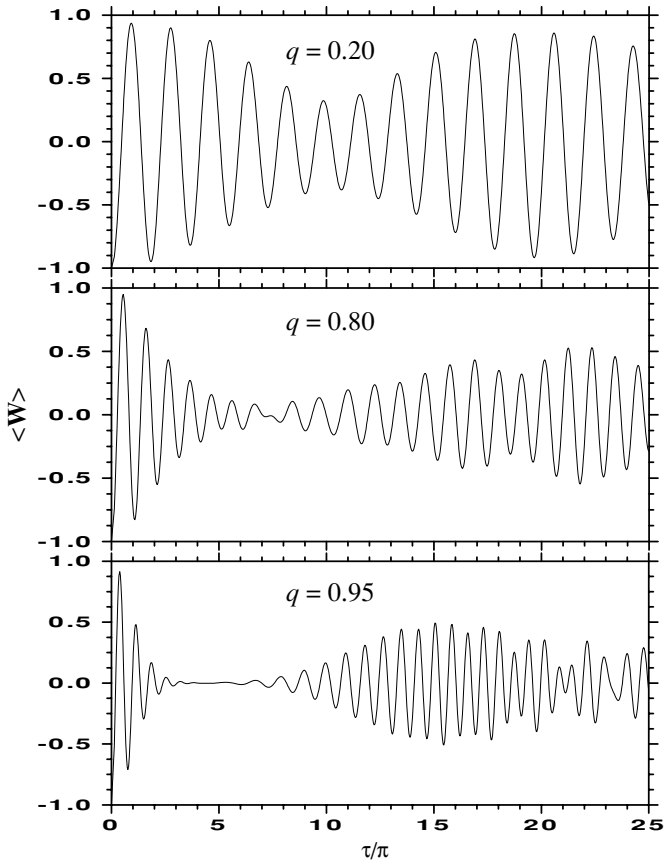

Figure 9. Time evolution of the population inversion factor $\langle \hat{\mathbf{W}}(t) \rangle$ for a self-similar coupling potential in the constant interaction case (x = u) with a pure initial state calculated for the scaling parameter values $q = 0.20, 0.80$ and 0.95. The values of the other constants are $|z|^2 = 10$, $R(a_1) = 1.0$ and $\Delta = 0.2$.

simplest case studied the remainder of equation (2.1) is given by $R(a_1) = ca_1$, where c is a constant. For this case one has

$$e_n = \left(\frac{1-q^n}{1-q}\right) R(a_1). \tag{6.16}$$

To get a specific form for the coherent state for this coupling potential, we define the functional $\mathcal{Z}_j$ as

$$\mathcal{Z}_j = R(a_1)\, \mathrm{e}^{-\mathrm{i}\alpha R(a_1)}, \tag{6.17}$$

where α is a real constant. We find that

$$\prod_{k=0}^{n-1} \mathcal{Z}_{j+k} = [R(a_1)]^n q^{n(n-1)/2}\, \mathrm{e}^{-\mathrm{i}\alpha e_n}. \tag{6.18}$$

Inserting (6.16) and (6.18) into (2.10) we can show that

$$h_n(a_r) = \rho^{-n} q^{-n^2/4} \sqrt{(q;q)_n}\, \mathrm{e}^{\mathrm{i}\alpha e_n}, \qquad \text{with} \quad \rho = \sqrt{\frac{R(a_1)(1-q)}{\sqrt{q}}}. \tag{6.19}$$

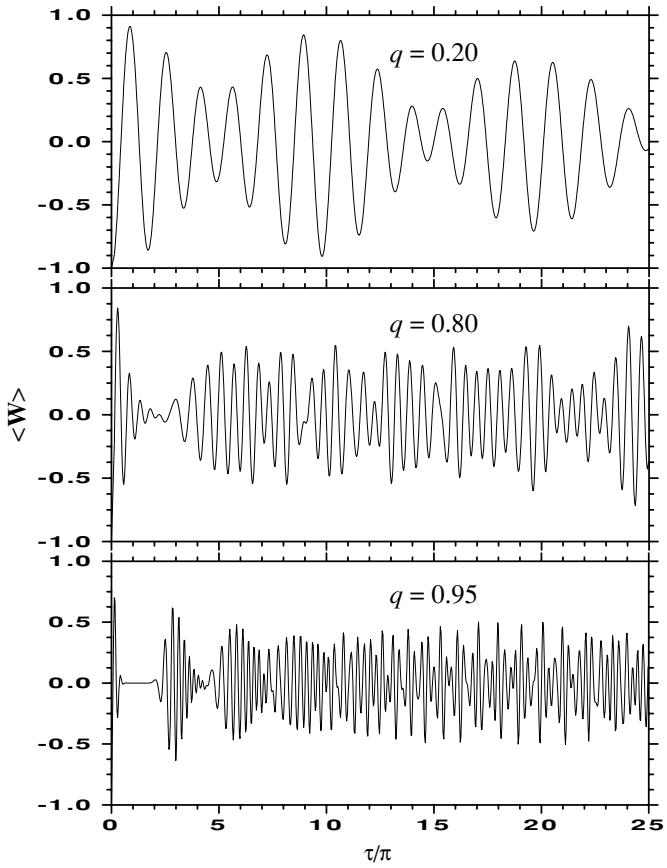

Figure 10. Same as figure 9, but for the intensity-dependent interaction case (x = i).

Using these results we obtain for the coherent state (2.9) and the expansion coefficient (5.9) the expressions [24]

$$|z;a_r\rangle = \sum_{n=0}^{\infty} \frac{q^{n^2/4}}{\sqrt{(q;q)_n}} \mathrm{e}^{-\mathrm{i}\alpha e_n} \xi^n |n\rangle, \qquad C_n = \frac{q^{n^2/2}|\xi|^{2n}}{(q;q)_n}, \tag{6.20}$$

where the q-shifted factorial $(q;q)_n$ is defined as $(p;q)_0 = 1$ and $(p;q)_n = \prod_{j=0}^{n-1}(1-pq^j)$, with $n \in \mathbb{Z}$, and $\xi = \rho z$. The quantities $\vartheta_n^{(\mathrm{x})}$ are given by

$$\vartheta_n^{(\mathrm{u})} = \sqrt{\left[\frac{R(a_1)(1-q^n)}{1-q}\right] + \Delta^2}, \qquad \text{and} \qquad \vartheta_n^{(\mathrm{i})} = \sqrt{\left[\frac{R(a_1)(1-q^n)}{1-q}\right]^2 + \Delta^2}. \tag{6.21}$$

For the pure initial state (4.4) we can use (6.20) and (6.21) into (5.12) and the definition of the one-parameter family of q-exponential functions [35, 36]

$$E_q^{(\mu)}(x) = \sum_{n=0}^{\infty} \frac{q^{\mu n^2}}{(q;q)_n} x^n, \qquad \text{with} \quad \mu \in \mathbb{R} \tag{6.22}$$

to get the expression for the weight distribution function

$$P^{(q)}(n,\xi) = \frac{q^{n^2/2}|\xi|^{2n}}{E_q^{(1/2)}(|\xi|^2)(q;q)_n}. \tag{6.23}$$

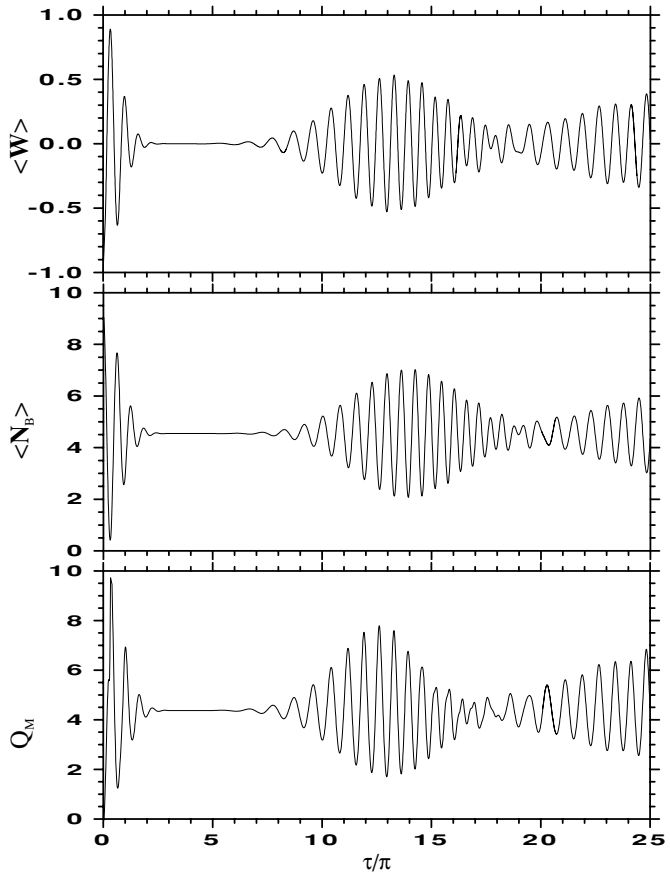

Figure 11. Time evolution of the dynamical variables for a self-similar coupling potential in the constant interaction case (x = u) for a pure initial state. The constant values used are $|z|^2 = 10$, $R(a_1) = 1.0$, $q = 0.99$ and $\Delta = 0.2$.

If we compare this expression with that one obtained for the harmonic oscillator coupling case we observe that (6.23) looks like the q-version of the Poissonian distribution (6.5), with the usual factorial $n!$ replaced by the q-shifted factorial $(q;q)_n$ and the exponential function $e^{-|z|^2}$ replaced by the q-exponential functions $E_q^{(1/2)}(|\xi|^2)$.

To see how the dynamical behaviour depends on the scaling parameter q we plot in figures 9 and 10 the population inversion factor $\langle\hat{\mathbf{W}}(t)\rangle$ for the constant (x = u) and intensity-dependent (x = i) interactions, respectively, for the values of the scaling parameter $q = 0.20, 0.80$ and 0.95. We assume a pure initial quantum state of the system. The set of other constants used is $|z|^2 = 10$, $R(a_1) = 1.0$ and $\Delta = 0.2$. For the standard coupling (x = u) the Rabi oscillations in $\langle\hat{\mathbf{W}}(t)\rangle$ show almost a regular pattern with a defined period and symmetric envelope. The frequency of the oscillations increases with the q value and only for higher values of this parameter the collapse and revival are complete. For the low and intermediate values of q the adjacent revivals present a strong overlapping and the final result in the Rabi oscillations and its envelope is an irregular pattern. When the interaction is intensity-dependent (x = i) $\langle\hat{\mathbf{W}}(t)\rangle$ and the scaling parameter q goes to unity (i.e., as we approach the harmonic oscillator limit) the revival events happen periodically. Each new revival event

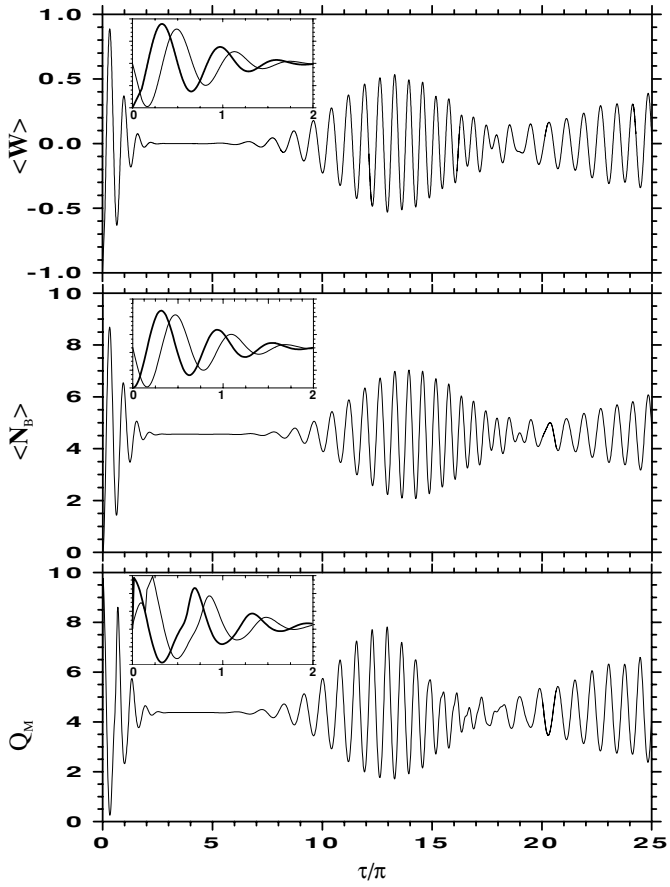

Figure 12. Same as figure 11 but for a mixed initial state of the system with $\beta\lambda = 1$. The insets display magnified views in time of the first collapse event for two different temperature values: $\beta\lambda = 1$ (thick line) and $\beta\lambda = 0$ (thin line).

shows more oscillations exhibiting a compression pattern in time with an irregular period. For the low and intermediate q values the time evolution of $\langle\hat{\mathbf{W}}(t)\rangle$ is very similar to what happens in the constant interaction case, but preserving its specific time oscillation properties. We conclude that the scaling parameter q has a fundamental importance on the phenomenon once its value defines the complete or incomplete nature of the collapse and revival of $\langle\hat{\mathbf{W}}(t)\rangle$. Only for higher values of the scaling parameter q (the harmonic oscillator limit) we observe a total collapse and revival of the population inversion factor.

Figures 11 and 12 display the results for the quantum dynamical variables for the constant (x = u) interaction case in terms of the time variable τ/π, when we have a pure and mixed initial state of the system, respectively. We take $q = 0.99$, $|z|^2 = 10$, $R(a_1) = 1$ and $\Delta = 0.2$. We note the increase in the collapse time of $\langle\hat{\mathbf{N}}_{\mathrm{B}}(t)\rangle$. As before the temperature effects on the dynamical variable behaviour are related to a time-shift. As in previous cases, the deformations in $Q_{\mathrm{M}}(t)$ manifest with a asymmetry in the envelopes of the oscillations. We find the critical coherent value of the Mandel parameter to be

$$Q_{\mathrm{ch}} = |z|^2 \left[\frac{R(a_1)}{q}\right]^2 \left\{\left[\frac{R(a_1)}{q}\right]^2 - 1\right\} + R(a_1) - 1 \tag{6.24}$$

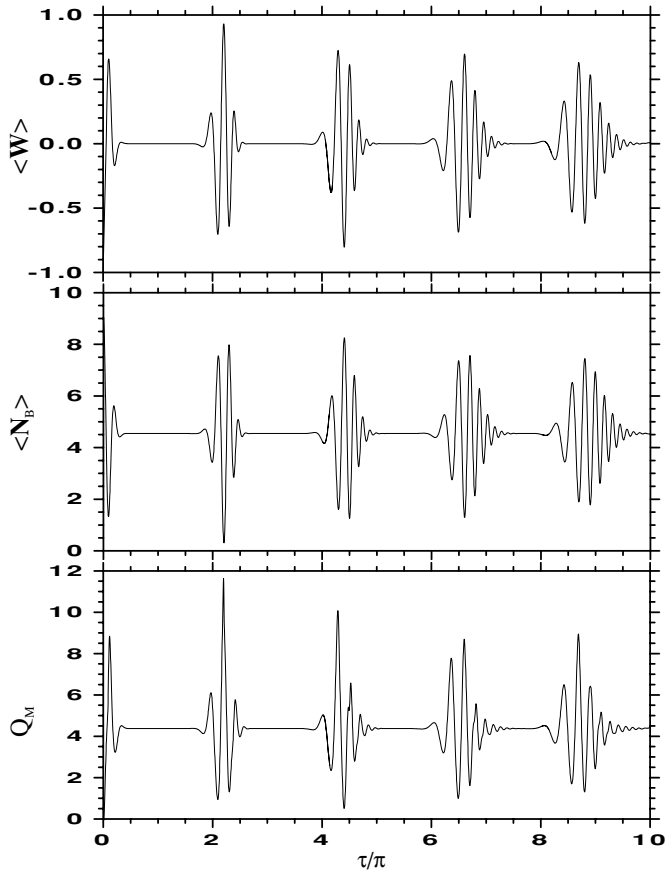

Figure 13. Same as figure 11, but for the intensity-dependent interaction case (x = i).

which, in the case of the constants used in this figure, gives the numerical value $Q_{\rm ch} = 0.21$. Therefore, except for short time intervals near $\tau = 0$, in general we find $Q_{\rm M}(t) > Q_{\rm ch}$ indicating that the coupling potential quantum states distribution is super-coherent.

Figures 13 and 14 are the versions of figures 11 and 12, respectively, for the intensity-dependent interaction (x = i) calculated with the same set of strengths. Note that in this case the Rabi oscillations of the quantum dynamical variables in the first revival events present almost a regular pattern with defined period and almost symmetric envelopes. Only for the following revival events the compression in the Rabi oscillations, the increase in the oscillation number and the asymmetry in the envelopes become more visible. In order to understand this behaviour of the dynamical variables we observe that in the limit $q \to 1$ we find $e_n \to nR(a_1)$ and $C_n \to |\sqrt{R(a_1)}z|^{2n}/n!$, therefore if we also use the limit [35, 36]

$$\lim_{q\to 1}\left\{E_q^{(\mu)}[(1-q)x]\right\} \to \mathrm{e}^x \tag{6.25}$$

it is possible to show that

$$\lim_{q\to 1} P^{(q)}(n,\xi) \longrightarrow \left(\frac{|z_1|^{2n}}{n!}\right)\mathrm{e}^{-|z_1|^2}, \qquad \text{where} \quad z_1 = \sqrt{R(a_1)}z \tag{6.26}$$

which corresponds to a Poisson distribution as we found in the harmonic oscillator coupling case. In other words, the dynamical behaviour for a self-similar coupling potential goes to that

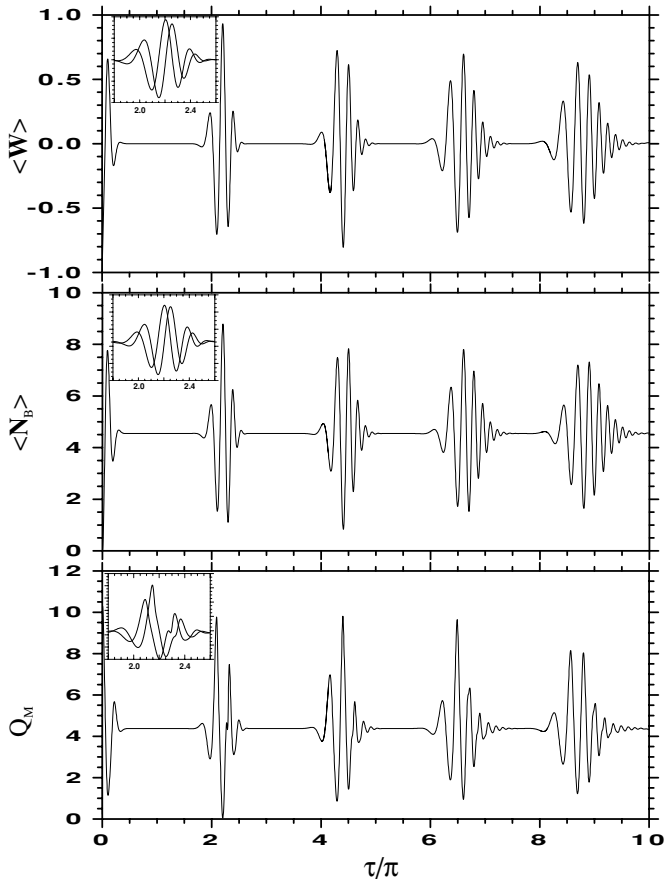

Figure 14. Same as figure 12, but for the intensity-dependent interaction case (x = i).

of the harmonic oscillator in the limit $q \to 1$. This similarity is gradually broken. It happens because for short time intervals the effects of the discrepancy between the value of $q = 0.99$ and the limit $q \to 1$ are less visible than for longer time intervals. Only for q values very close to 1 we see the exact harmonic oscillator dynamics. It is remarkable that in the case of the self-similar coupling potential, because of the introduction of an additional variable (the scaling parameter q), we have a richer dynamical behaviour with the appearance of new and interesting properties.

We must again emphasize that the set of system parameters used to get our results in this case was also chosen with the intention to make evident the collapse and revival phenomenon in the physical quantities. We observed that the collapse and revival times are basically defined by the value of q. As in the other applications, the detuning Δ parameter defines the temporal position of the whole oscillatory pattern, without distortions.

Finally we point out that in our discussion we avoided using analytic approximations, such as the use of the saddle-point approach [26, 29]. Such analytic expressions are strongly dependent on the coherent state coupling potential specific form and, as we showed in the [24] there is a generalized way to construct coherent states for shape-invariant potentials. In the case of the harmonic oscillator various approaches are equivalent resulting in the same

final expression for $|z\rangle$. However in the case of other shape-invariant coupling potentials this clearly is not the case and justification of analytical approaches is difficult.

7. Conclusions

Exactly soluble and fully quantum-mechanical models are rare. In this paper, we introduced a class of shape-invariant bound-state problems which represent two-level systems coupled with shape-invariant potentials. This represents a non-trivial coupled-channel problem which may find applications in molecular, atomic and nuclear physics. Taking into account two possible forms of coupling interaction (constant and intensity-dependent), and two possible initial quantum states of the system (pure or mixed states) we obtained the wavefunction and the density operator of the system. With this we obtained generalized expressions for some dynamical variables of the system, such as the population inversion factor $\langle \hat{\mathbf{W}}(t) \rangle$, the intensity of the shape-invariant coupling $\langle \hat{\mathbf{N}}_{\mathrm{B}}(t) \rangle$ and the Mandel parameter $Q_{\mathrm{M}}(t)$. We studied the behaviour of these dynamical variables for three different kinds of shape-invariant coupling potentials (harmonic oscillator, Pöschl–Teller and self-similar potentials). The results found in these applications exhibit rapid oscillations which periodically collapse and regenerate in different ways, depending on the nature of the coupling potential. Both collapse and revival events observed are purely quantum effects resulting from the discreteness of the coupling potential spectra. For shape-invariant coupling potentials other than the harmonic oscillator the collapses and revivals show some new and interesting properties such as non-regular Rabi oscillations with undefined periods; revivals with asymmetric wing envelopes and increases in the Rabi oscillation numbers. This quantum phenomenon of decay and regeneration is well known in a few restricted cases for the population inversion factor when we have harmonic oscillator coupling potentials. Our results confirm that the occurrence of this interesting quantum phenomenon is not restricted to the population inversion factor but is shared by the other quantum dynamical variables and is related to the model properties, like the kind of interaction and the coherent state associated with the coupling potential. It is remarkable that in the case of the self-similar coupling potential we have a wide range of behaviours: the scaling parameter q has a fundamental importance on the dynamical variable since its value defines the complete or incomplete nature of the collapse and revival events.

Acknowledgments

This work was supported in part by the US National Science Foundation Grant nos INT-0070889 and PHY-0244384 at the University of Wisconsin, and in part by the University of Wisconsin Research Committee with funds granted by the Wisconsin Alumni Research Foundation. ANFA is grateful to Paulo Carrilho S Filho and Pedro C Guaranho for valuable help and hints in numerical calculations and thanks the Nuclear Theory Group at University of Wisconsin for their very kind hospitality.

References

[1] Witten E 1981 *Nucl. Phys.* B **185** 513
For a recent review see Cooper F, Khare A and Sukhatme U 1995 *Phys. Rep.* **251** 267
[2] Gendenshtein L 1983 *Pis'ma Zh. Eksp. Teor. Fiz.* **38** 299
Gendenshtein L 1983 *JETP Lett.* **38** 356
[3] Cooper F, Ginocchio J N and Khare A 1987 *Phys. Rev.* D **36** 2458
[4] Balantekin A B 1998 *Phys. Rev.* A **57** 4188

[5] Chaturvedi S, Dutt R, Gangopadhyay A, Panigrahi P, Rasinariu C and Sukhatme U 1998 *Phys. Lett.* A **248** 109
[6] Balantekin A B, Cândido Ribeiro M A and Aleixo A N F 1999 *J. Phys. A: Math. Gen.* **32** 2785
[7] Dutt R, Gangopadhyay A and Sukhatme U 1997 *Am. J. Phys.* **65** 400
[8] Choi J-Y and Hong S-I 1999 *Phys. Rev.* A **60** 796
[9] Dunne G and Feinberg J 1998 *Phys. Rev.* D **57** 1271
[10] Freedman D Z and Mende P F 1990 *Nucl. Phys.* B **344** 317
[11] Khare A and Bhaduri R K 1994 *J. Phys. A: Math. Gen.* **27** 2213
[12] Ghosh P K, Khare A and Sivakumar M 1998 *Phys. Rev.* A **58** 821
[13] Amado R D, Cannata F and Dedonder J-P 1988 *Phys. Rev.* A **38** 3797
Amado R D, Cannata F and Dedonder J-P 1990 *Int. J. Mod. Phys.* A **5** 3401
Das T K and Chakrabarti B 1999 *J. Phys. A: Math. Gen.* **32** 2387
[14] Balantekin A B and Takigawa N 1998 *Rev. Mod. Phys.* **70** 77
Hagino K and Balantekin A B 2004 *Phys. Rev.* A **70** 032106
[15] Aleixo A N F, Balantekin A B and Cândido Ribeiro M A 2000 *J. Phys. A: Math. Gen.* **33** 3173
[16] Aleixo A N F, Balantekin A B and Cândido Ribeiro M A 2001 *J. Phys. A: Math. Gen.* **34** 1109
[17] Jaynes E T and Cummings F W 1963 *Proc. IEEE* **51** 89
[18] Allen L and Eberly J H 1975 *Optical Resonance and Two-Level Atoms* (New York: Wiley)
Schleich W P 2001 *Quantum Optics in Phase Space* (Berlin: Wiley)
[19] Frasca M 2003 *Ann. Phys.* **306** 193
[20] Aleixo A N F, Balantekin A B and Cândido Ribeiro M A 2002 *J. Phys. A: Math. Gen.* **35** 9063
[21] Chuan C 1991 *J. Phys. A: Math. Gen.* **24** L1165
[22] Khare A and Sukhatme U 1994 *J. Phys. A: Math Gen.* **26** L901
Barclay D T, Dutt R, Gangopadhyaya A, Khare A, Pagnamenta A and Sukhatme U 1993 *Phys. Rev.* A **48** 2786
[23] Klauder J R and Skagerstam B S 1985 *Coherent States—Applications in Physics and Mathematical Physics* (Singapore: World Scientific)
Perelomov A M 1986 *Generalized Coherent States and Their Applications* (Berlin: Springer)
[24] Aleixo A N F and Balantekin A B 2004 *J. Phys. A: Math. Gen.* **37** 8513
[25] Glauber R J 1963 *Phys. Rev.* **130** 2529
Glauber R J 1963 *Phys. Rev.* **131** 2766
[26] Buck B and Sukumar C V 1981 *Phys. Lett.* A **81** 132
Buck B and Sukumar C V 1984 *J. Phys. A: Math. Gen.* **17** 885
[27] Gou S-C 1990 *Phys. Lett.* A **147** 218
[28] Rybin A, Miroshnichenko G, Vadeiko I and Timonen J 1999 *J. Phys. A: Math. Gen* **32** 8739
[29] Eberly J H, Narozhny N B and Sanchez-Mondragon J J 1980 *Phys. Rev. Lett.* **44** 1323
Eberly J H, Narozhny N B and Sanchez-Mondragon J J 1981 *Phys. Rev.* A **23** 236
Yoo H-I, Sanchez-Mondragon J J and Eberly J H 1981 *J. Phys. A: Math. Gen.* **14** 1383
[30] Buzek V 1989 *Phys. Rev.* A **39** 3196
Gerry C C 1988 *Phys. Rev.* A **37** 2683
Singh S 1982 *Phys. Rev.* A **25** 3206
[31] Cirac J I, Blatt R, Parkins A S and Zoller P 1994 *Phys. Rev.* A **49** 1202
[32] Smith D S Multiple precision computation home-page: http://myweb.lmu.edu/dmsmith/FMLIB.html; web search keyword: *dsmithfmlibrary*
[33] Fukui T and Aizawa N 1994 *Phys. Lett.* A **189** 7
[34] Shabat A B 1992 *Inverse Problem* **8** 303
Spiridonov V 1992 *Phys. Rev. Lett.* **69** 398
[35] Floreanini R, LeTourneux J and Vinet L 1995 *J. Phys. A: Math. Gen.* **28** L287
[36] Atakishiyev N M 1996 *J. Phys. A: Math. Gen.* **29** L223
Exton H 1983 *q-Hypergeometric Functions and Applications* (Chichester: Ellis Horwood)